Image-Based Aspect Ratio Selection

– Supplementary Material –

Yunhai Wang, Zeyu Wang, Chi-Wing Fu, Hansjörg Schmauder, Oliver Deussen and Daniel Weiskopf

This supplemental material file provides additional experimental and evaluation results for our submitted paper titled "Image-Based Aspect Ratio Selection." In summary, it includes the following four parts:

- First, we provided the detailed derivations of imgAWO and imgRV (Section 1).
- Hereafter, we employed all six aspect ratio selection methods discussed in our paper (i.e., imgRV, imgAL, imgAWO, isoRV, isoAL, and isoAWO) and compared their performance on both deviations (see main paper for its definition) and the method runtime (Section 2).
- Furthermore, we conducted a complete comparison between imgRV and the six criterions presented in [5] using all the datasets appeared in their paper and supplemental material [5] (Section 3).
- Finally, we presented additional results produced from our method (Section 4).

- *Y. Wang and Z. Wang are with Shandong University. Email: {cloudseawang,zywangx}@gmail.com. Y. Wang and Z. Wang are joint first authors.*
- *C.-W. Fu is with the Chinese University of Hong Kong. E-mail: cwfu@cse.cuhk.edu.hk.*
- *O. Deussen is with Konstanz University and Shenzhen VisuCA Key Lab, SIAT, China. E-mail: oliver.deussen@uni-konstanz.de.*
- *H. Schmauder and D. Weiskopf are with VISUS, University of Stuttgart, Germany. E-mail: {hansjoerg.schmauder, Daniel.Weiskopf}@visus.uni-stuttgart.de.*

Manuscript received xx xxx. 201x; accepted xx xxx. 201x. Date of Publication xx xxx. 201x; date of current version xx xxx. 201x. For information on obtaining reprints of this article, please send e-mail to: reprints@ieee.org. Digital Object Identifier: xx.xxxx/TVCG.201x.xxxxxxx

1 Deriving imgAWO and imgRV

In this appendix, we present the details for deriving the formulations for imgAWO and imgRV:

ImgAWO. Since Eq. (7) is not a single line integral as for AL, we cannot directly apply Eq. (6) to Eq. (7). However, by considering C in each line integral term (see the numerator and denominator in Eq. (7)) as the set of all isolines over all isovalues, i.e., $C = \{C_t\}\ \forall t \in [0,1]$, we can rewrite the numerator and denominator in Eq. (7) as

$$\min_{\alpha\in(0,\infty)} \left| \frac{\int_0^1 \int_{C_t} |\theta(\alpha)|\,\mathrm{d}s\,\mathrm{d}t}{\int_0^1 \int_{C_t} \mathrm{d}s\,\mathrm{d}t} - \frac{\pi}{4} \right|, \tag{1}$$

and then apply Eq. (6) to each line integral term by putting $f = |\theta(\alpha)|$ and $f = 1$ into Eq. (6). For the line integral with $f = 1$, the right hand side of Eq. (6) can be easily obtained. For the line integral with $f = |\theta(\alpha)|$, we consider the local tangent vector in Ω_α, i.e., $(\frac{1}{\alpha}\frac{\partial\rho}{\partial y}, -\frac{\partial\rho}{\partial x})$, which is always perpendicular to the local gradient vector from Eq. (5); see the inset figure on the right. Hence, the local orientation (tangent) θ along the isoline can be expressed as:

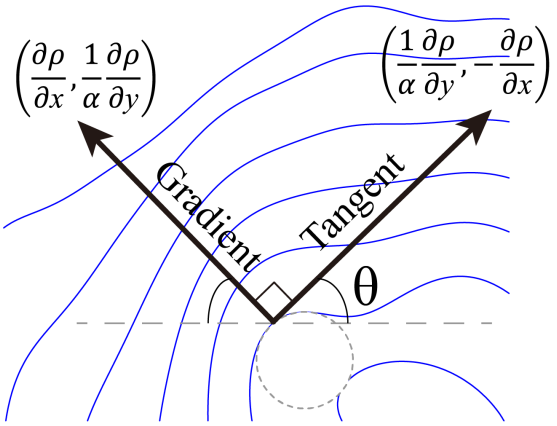

$$\theta = \tan^{-1}\left(\frac{-\frac{\partial\rho}{\partial x}}{\frac{1}{\alpha}\frac{\partial\rho}{\partial y}} \right), \text{ so } |\theta| = \tan^{-1}\left(\alpha \frac{\partial\rho}{\partial x} / \frac{\partial\rho}{\partial y} \right). \tag{2}$$

Putting the above results and Eq. (7) together, we can obtain the objective of imgAWO as shown in Eq. (8).

ImgRV. Given the line integral form of RV presented in Eq. (9), we, again, consider $C = \{C_t\}\ \forall t \in [0,1]$ and rewrite Eq. (9) as

$$\alpha = \frac{\int_0^1 \int_{C_t} |\cos(\theta)|\,\mathrm{d}s\,\mathrm{d}t}{\int_0^1 \int_{C_t} |\sin(\theta)|\,\mathrm{d}s\,\mathrm{d}t}. \tag{3}$$

We can then apply Eq. (6) to each line integral in the numerator and denominator, and obtain

$$\alpha = \frac{\int_{\Omega_{1.0}} |\cos(\theta)|\,||(\frac{\partial\rho}{\partial x}, \frac{\partial\rho}{\partial y})||\,\mathrm{d}x\,\mathrm{d}y}{\int_{\Omega_{1.0}} |\sin(\theta)|\,||(\frac{\partial\rho}{\partial x}, \frac{\partial\rho}{\partial y})||\,\mathrm{d}x\,\mathrm{d}y}. \tag{4}$$

By further considering the local gradient $(\frac{\partial\rho}{\partial x}, \frac{\partial\rho}{\partial y})$ and its corresponding tangent vector $(\frac{\partial\rho}{\partial y}, -\frac{\partial\rho}{\partial x})$ in $\Omega_{1.0}$, we can simplify Eq. (4), and obtain the formulation of imgRV as presented in Eq. (10).

In addition, there are the equations (presented in our paper) mentioned above:

$$\nabla\rho_\alpha(\mathbf{x}) = \left(\frac{\partial\rho}{\partial x}, \frac{1}{\alpha}\frac{\partial\rho}{\partial y}\right), \tag{5}$$

$$\int_0^1 \left(\int_{L_\alpha(t)} f(\mathbf{X},\alpha)\,\mathrm{d}s \right) \mathrm{d}t = \int_{\Omega_{1.0}} f(\mathbf{X},\alpha) \left|\left| \left(\alpha\frac{\partial\rho}{\partial x}, \frac{\partial\rho}{\partial y}\right) \right|\right| \mathrm{d}x\,\mathrm{d}y, \tag{6}$$

$$\min_{\alpha\in(0,\infty)} \left| \frac{\int_C |\theta(\alpha)|\mathrm{d}s}{\int_C \mathrm{d}s} - \frac{\pi}{4} \right|. \tag{7}$$

$$\min_{\alpha\in(0,\infty)} \left| \frac{\int_D \left|\tan^{-1}\left(\frac{\partial\rho}{\partial x}/\frac{\partial\rho}{\alpha\partial y}\right)\right| \left|\left|\left(\alpha\frac{\partial\rho}{\partial x}, \frac{\partial\rho}{\partial y}\right)\right|\right| \mathrm{d}x\,\mathrm{d}y}{\int_D \left|\left|\left(\alpha\frac{\partial\rho}{\partial x}, \frac{\partial\rho}{\partial y}\right)\right|\right| \mathrm{d}x\,\mathrm{d}y} - \frac{\pi}{4} \right|, \tag{8}$$

$$\alpha = \frac{\sum_i |\Delta x_i|}{\sum_i |\Delta y_i|} = \frac{\int_C |\cos\theta|\,\mathrm{d}s}{\int_C |\sin\theta|\,\mathrm{d}s}. \tag{9}$$

$$\alpha = \frac{\int_{\Omega_{1.0}} ||\frac{\partial\rho}{\partial y}||\,\mathrm{d}x\,\mathrm{d}y}{\int_{\Omega_{1.0}} ||\frac{\partial\rho}{\partial x}||\,\mathrm{d}x\,\mathrm{d}y}, \tag{10}$$

2 Comprehensive Comparison with more Aspect Ratio Selection Methods

The overall results of the deviation measure comparing with isoRV for all the six methods are shown in Figure 1(a). Note that the number of isovalues (m) is 1000 for isoline-based methods, if we want to ensure high precision. We generate the boxplots by applying the 100 datasets described in Section 6.1 of our paper. It is obvious to show that our imgRV method selects the most similar result with isoRV compared to all other methods. Figure 1(b) summarizes and compares the time performance of the six methods, where $m = 500$ is used here for keeping the consistency with the paper; this result clearly shows that imgRV is the fastest method. Furthermore, more details can be found in Appendices A and B for all dataset comparisons between the methods with m set to be 100 and 500, respectively.

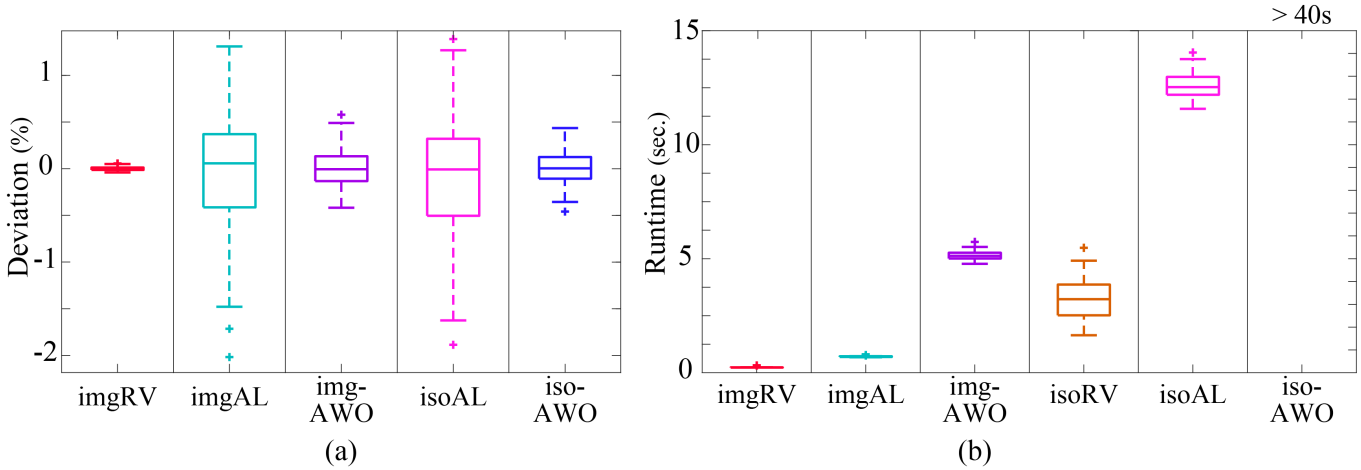

Fig. 1: Comprehensive comparison of the six methods. (a) Deviation of aspect ratios selected by our image-based methods (imgRV, imgAL, and imgAWO) and two isoline-based methods (isoAL and isoAWO, with 1000 isovalues) from those selected by isoRV (with 1000 isovalues); and (b) runtime of our methods and the three isoline-based methods (with 500 isovalues) for aspect ratio selection.

3 Comparison with All Six Criteria in Fink et al.

Figures 2, 3, and 4 show the comparison with more datasets [3, 11, 7, 6, 10, 5].

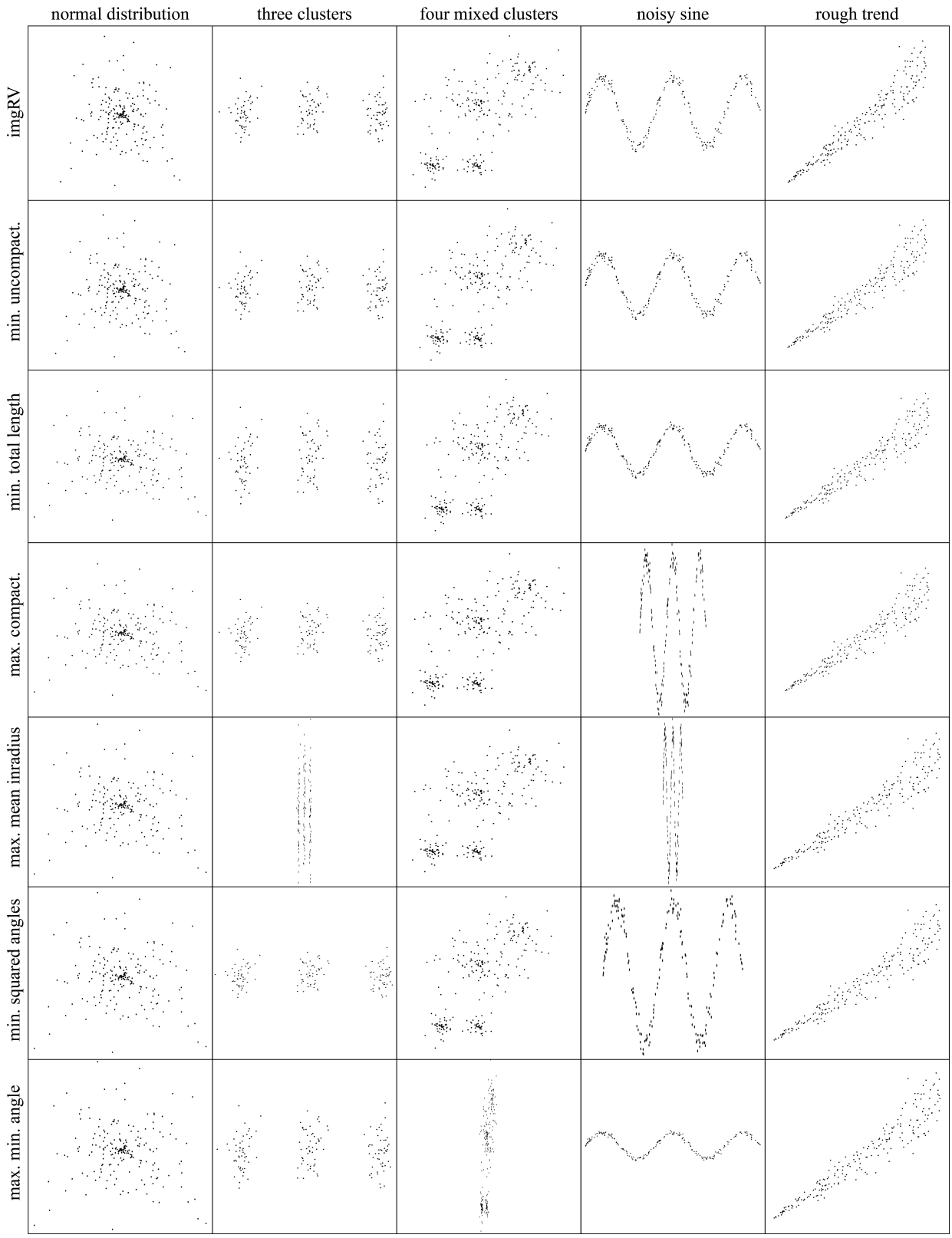

Fig. 2: Comparison between imgRV and the six methods of Fink et al. [5]: (1) minimizing uncompactness, (2) minimizing total length, (3) maximizing compactness, (4) maximizing mean inradius, (5) minimizing squared angles, and (6) maximizing minimum angle, over the five synthesized datasets.

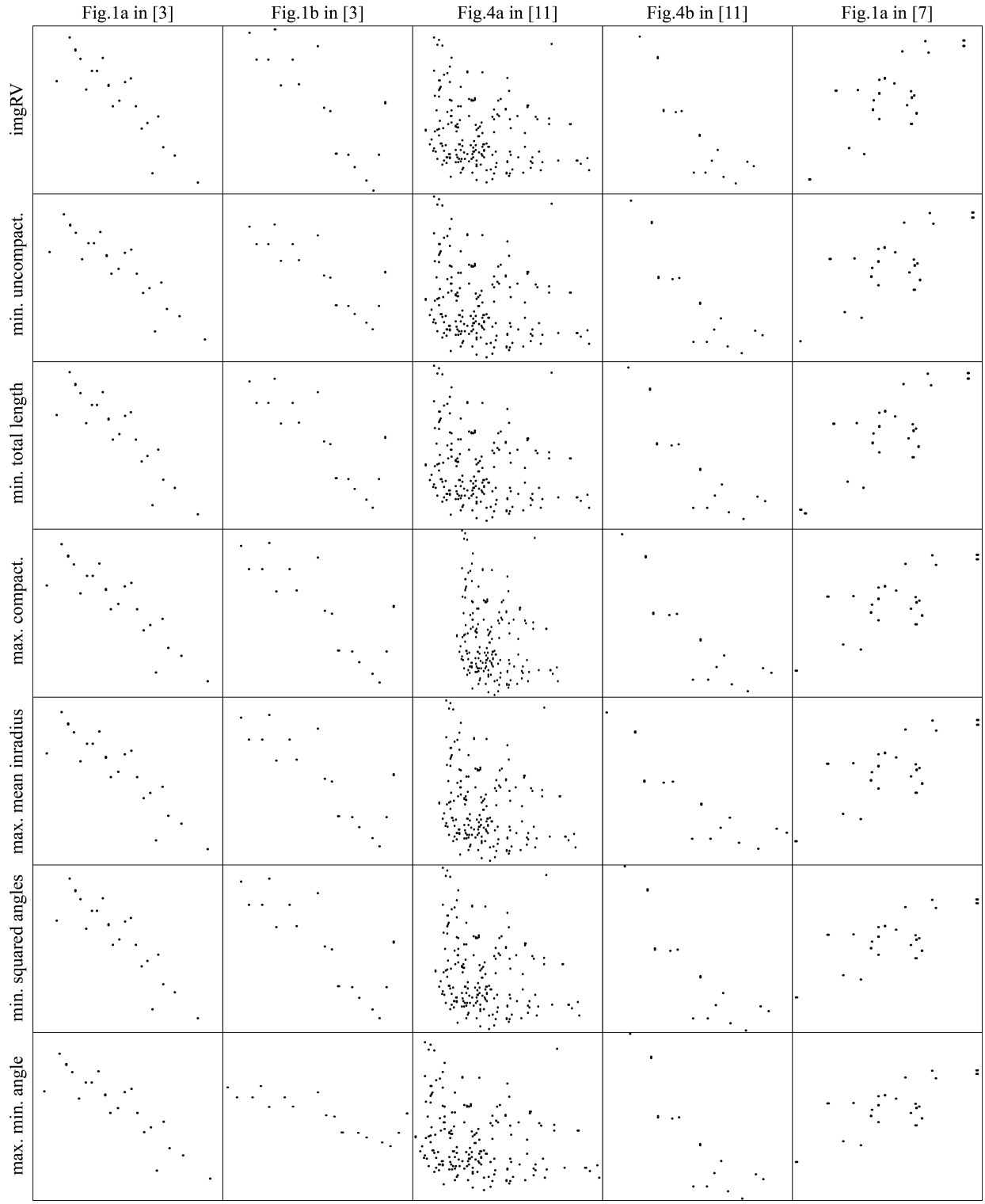

Fig. 3: Comparison between imgRV and the six methods of Fink et al. [5]: (1) minimizing uncompactness, (2) minimizing total length, (3) maximizing compactness, (4) maximizing mean inradius, (5) minimizing squared angles, and (6) maximizing minimum angle, over five datasets from *Nature* papers [3, 11, 7].

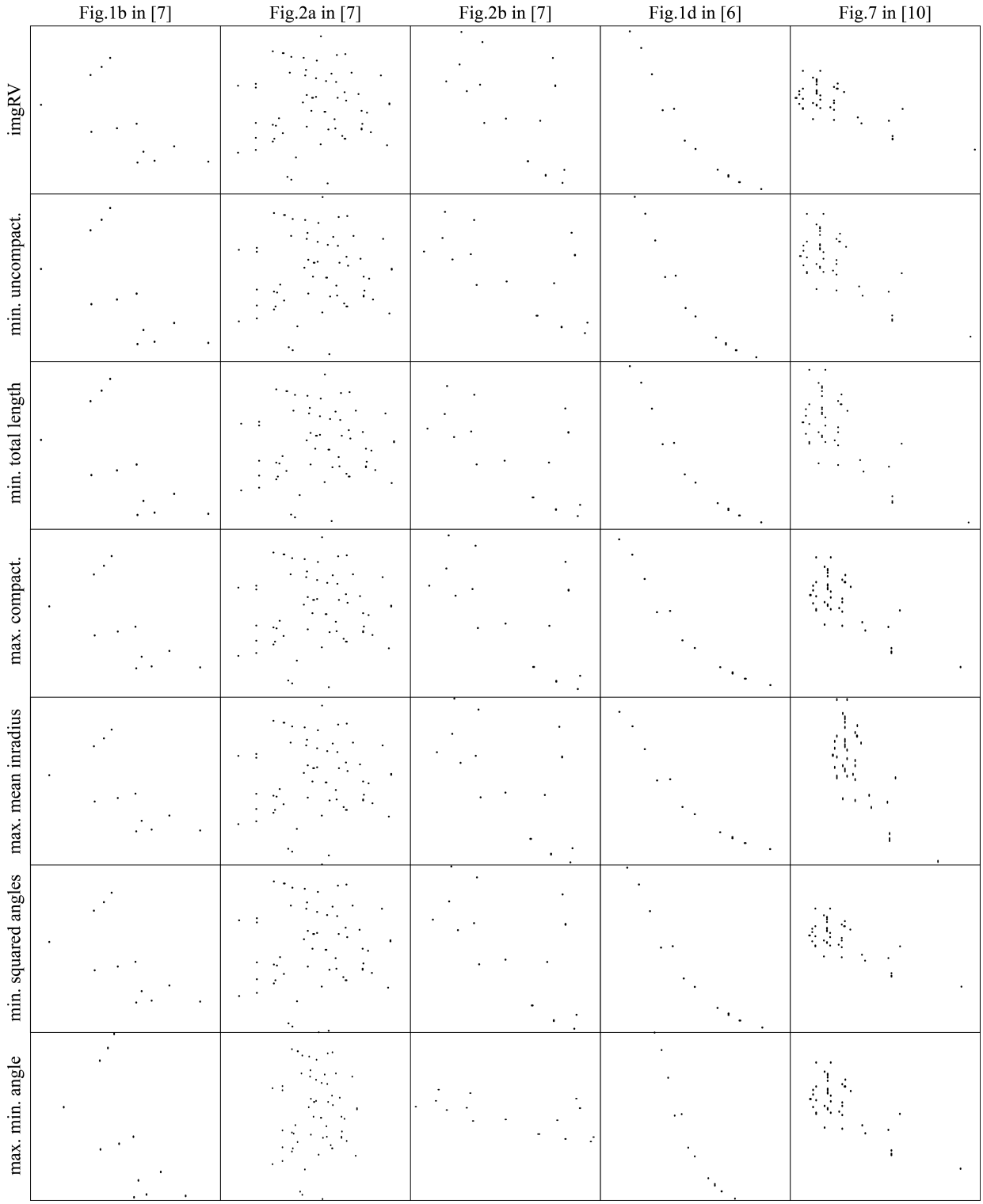

Fig. 4: Comparison between imgRV and the six methods of Fink et al. [5]: (1) minimizing uncompactness, (2) minimizing total length, (3) maximizing compactness, (4) maximizing mean inradius, (5) minimizing squared angles, and (6) maximizing minimum angle, over five datasets from *Nature* and *TVCG* papers [7, 6, 10].

4 Additional Results from Our Method

Additional results are provided in this section.

4.1 Region-of-Interest (ROI) Banking

Figures 5 and 6 present two ROI banking results.

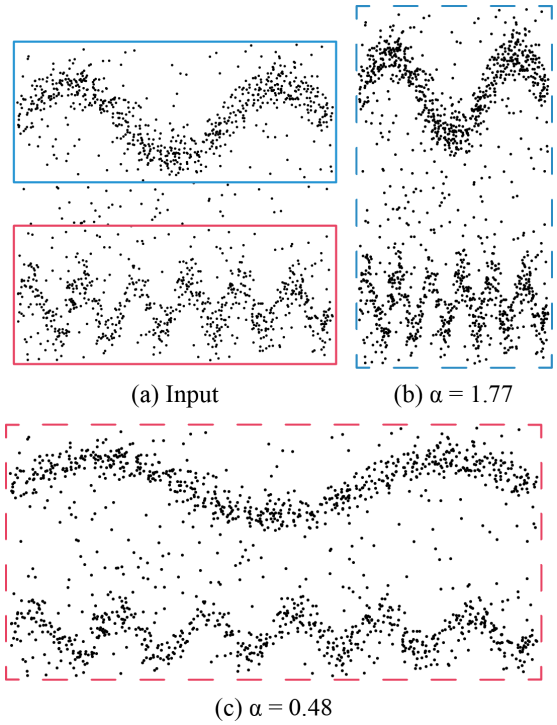

Fig. 5: ROI banking on the scatterplot with two different sine-trend clusters and random noise points. Our method can take user-specified ROIs (red and blue boxes in (a)) as inputs and select aspect ratios (b, c) that focus on revealing patterns inside.

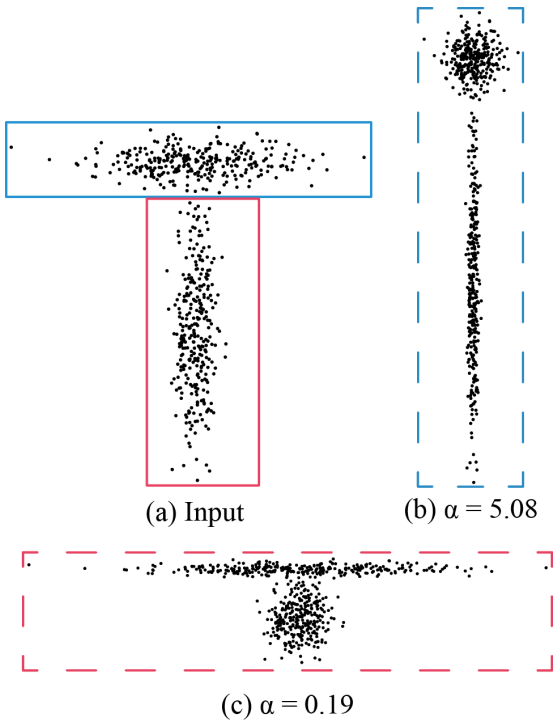

Fig. 6: ROI banking on the scatterplot of two Gaussian clusters. Our method can take user-specified ROIs (red and blue boxes in (a)) as inputs and select aspect ratios (b, c) that focus on revealing patterns inside.

4.2 Multi-Scale Banking

Figure 7 shows another instance of our multi-scale banking result with the *Twosquare* dataset [9].

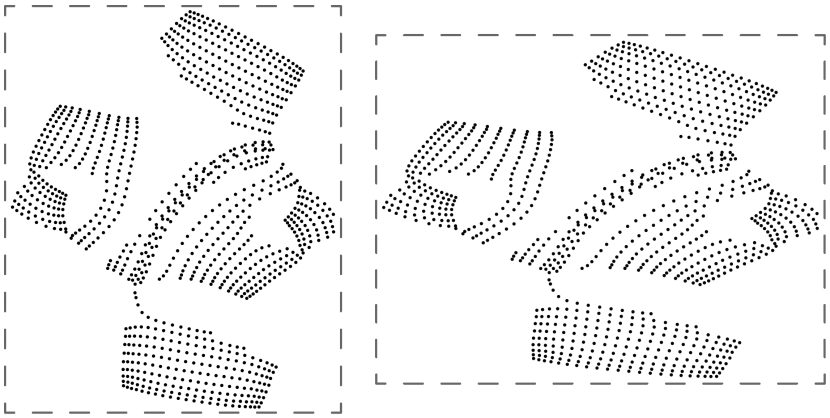

Fig. 7: Multi-scale banking on the *Twosquare* dataset [9]. Two aspect ratios are picked to show patterns of interest at different scales.

4.3 Image Data

Moreover, we generate more results by selecting aspect ratios for different images from internet in Figure 8 for the typical temperature dataset at Shawnigan Lake [8] and Figure 9 for the daily average temperatures dataset of New York, San Francisco and Austin [2].

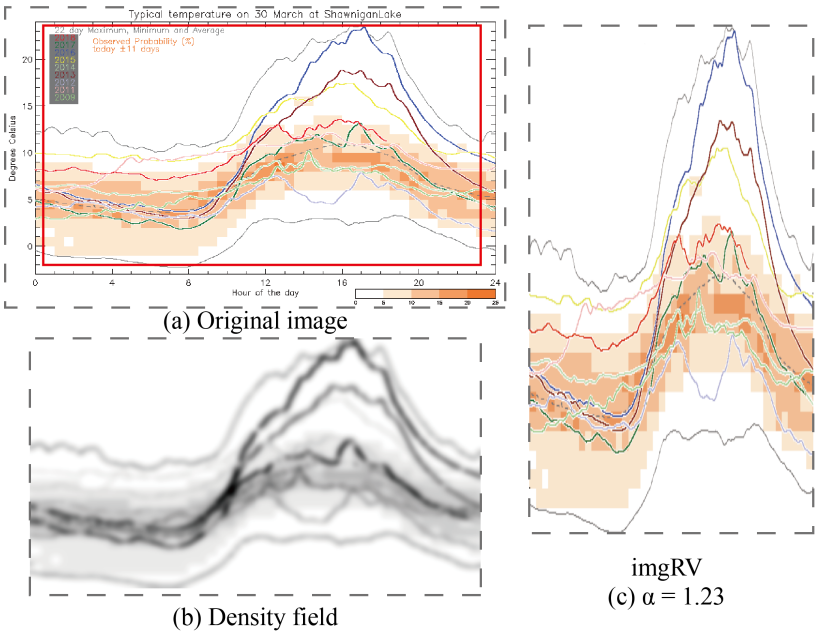

Fig. 8: Selecting a good aspect ratio for an image from the Internet [8]: (a) crop a relevant image part; (b) density field converted from the cropped image; and (c) result plotted with our selected aspect ratio.

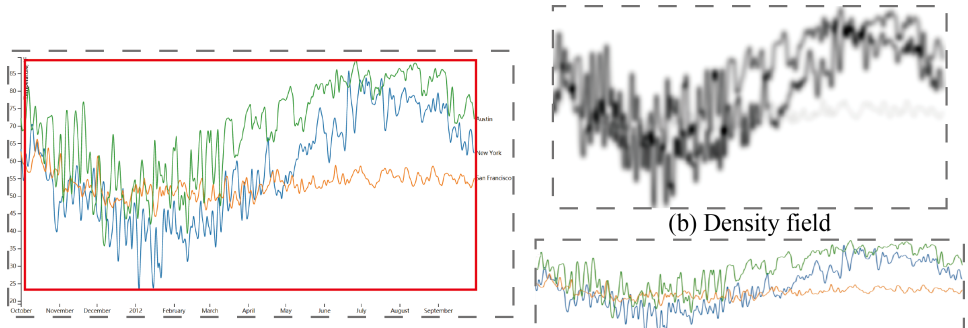

Fig. 9: Selecting a good aspect ratio for an image from the Internet [2]: (a) crop a relevant image part; (b) density field converted from the cropped image; and (c) result plotted with our selected aspect ratio.

4.4 Density Function Plots

Finally, three examples of density function plots are presented in Figure 10 for the *blunt-fin* dataset [1], Figure 11 for the *Turbulent* dataset [12], and Figure 12 for the *Feet* dataset [12].

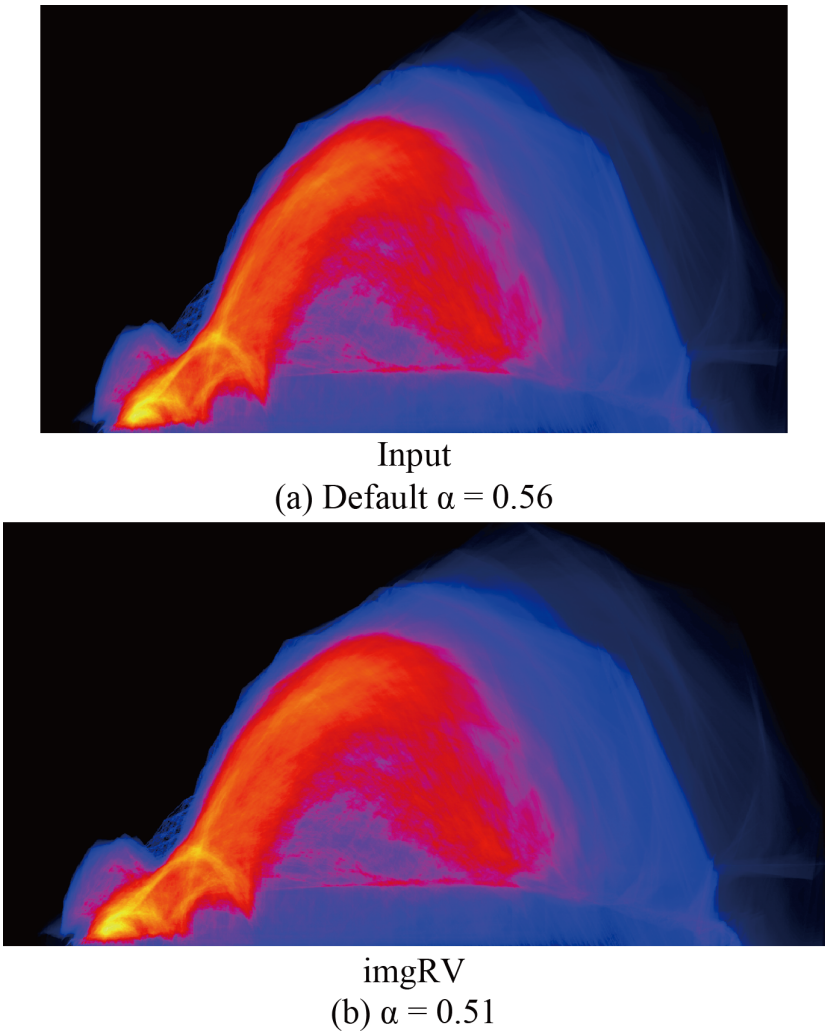

Fig. 10: Selecting an aspect ratio directly from a density function plot. (a) The input dataset is a continuous scatterplot of the *blunt-fin* dataset [1]. (b) Rescaled using a selected by imgRV.

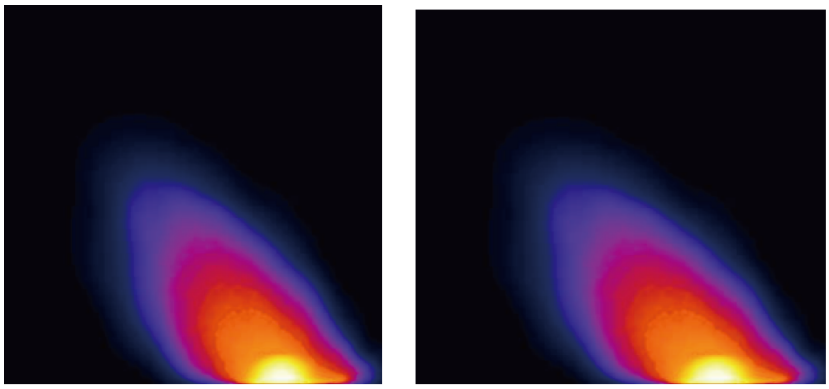

Input
(a) Default α = 1.0

imgRV
(b) α = 0.91

Fig. 11: Selecting an aspect ratio directly from a density function plot. (a) The input dataset is a continuous scatterplot of the *Turbulent* dataset [12]. (b) Rescaled using a selected by imgRV.

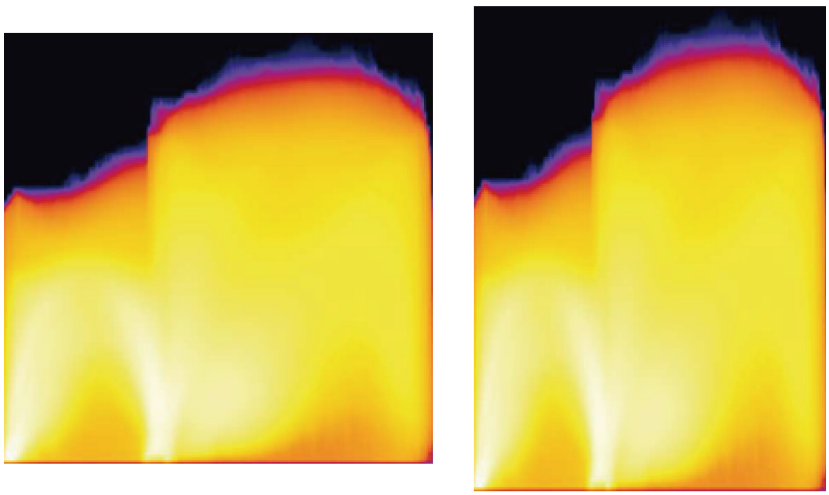

Input
(a) Default α = 1.0

imgRV
(b) α = 1.36

Fig. 12: Selecting an aspect ratio directly from a density function plot. (a) The input dataset is a continuous scatterplot of the *Feet* dataset [12]. (b) Rescaled using a selected by imgRV.

4.5 Effect of k in Anisotropic KDE

In addition, we present two examples to show the influence of the number of nearest neighbors (k) on the constructed anisotropic density field and the aspect ratios selected by imgRV in Figure 13 for the *Interleaved* dataset [9] and in Figure 14 for the *Statlog Image Segmentation* dataset [4].

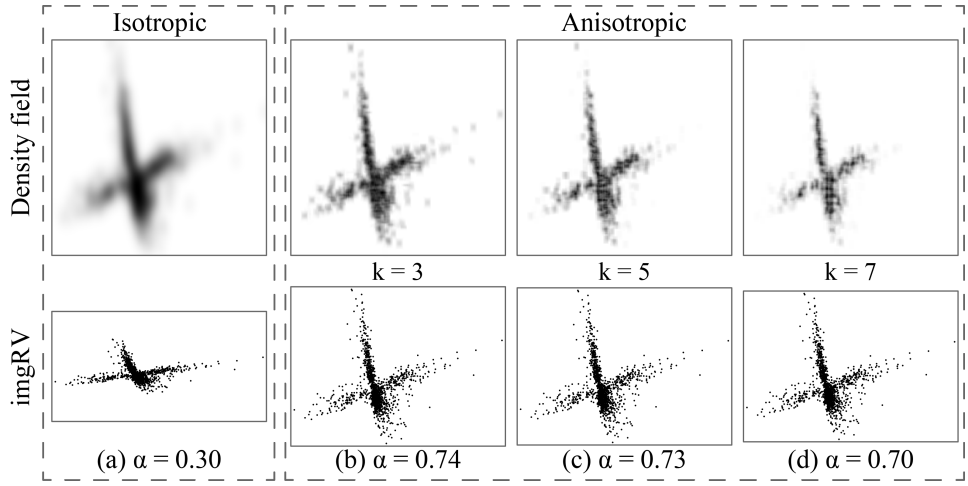

Fig. 13: Influence of the number of nearest neighbors (k) on the constructed anisotropic density field and the aspect ratios selected by imgRV on the *Interleaved* dataset [9]. (a) Density field constructed by isotropic KDE and its resulting plot; (b, c, d) density fields constructed by anisotropic KDE with different k and the resulting plots.

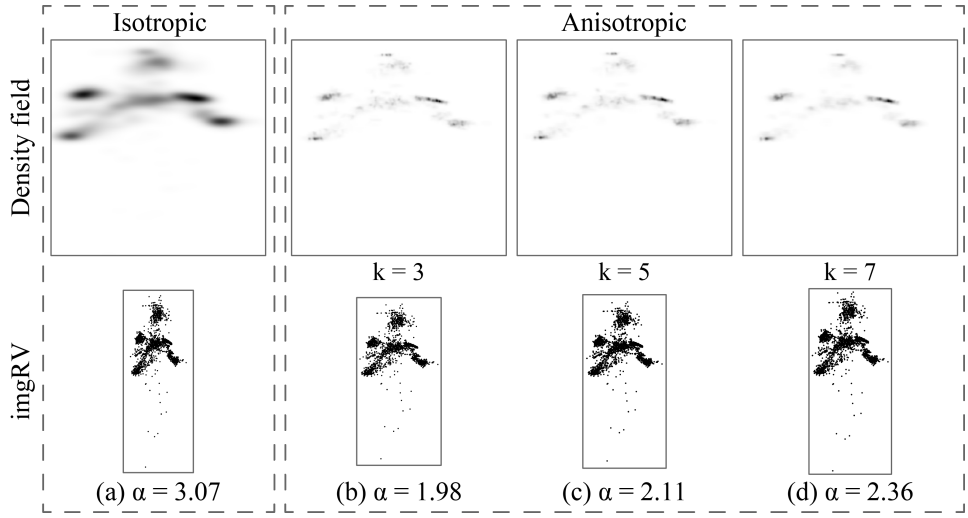

Fig. 14: Influence of the number of nearest neighbors (k) on the constructed anisotropic density field and the aspect ratios selected by imgRV on the *Statlog Image Segmentation* dataset [4]. (a) Density field constructed by isotropic KDE and its resulting plot; (b, c, d) density fields constructed by anisotropic KDE with different k and the resulting plots.

APPENDIX A: COMPREHENSIVE COMPARISON OF SIX METHODS WITH 100 ISOVALUES

In this appendix, we present the detailed results with all 100 datasets from [4, 9] for comprehensive comparison of the six methods described in Section 2. Note that the number of isovalues $m = 100$. Moreover, the results whose deviations with isoRV (with $m = 1000$) are larger than 10% are plotted with a red bounding box.

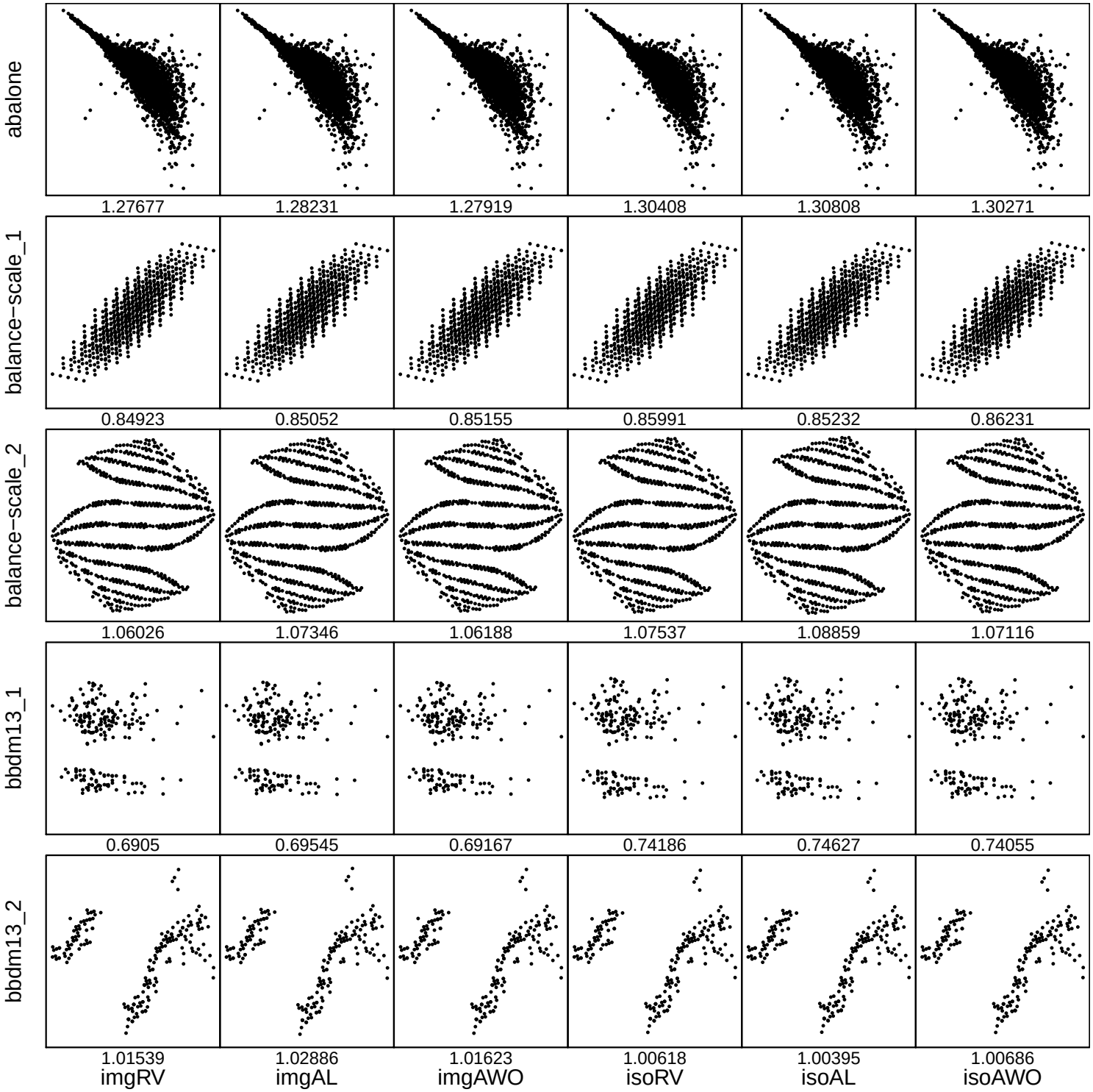
abalone
balance−scale_1
balance−scale_2
bbdm13_1
bbdm13_2
1.27677
1.28231
1.27919
1.30408
1.30808
1.30271
0.84923
0.85052
0.85155
0.85991
0.85232
0.86231
1.06026
1.07346
1.06188
1.07537
1.08859
1.07116
0.6905
0.69545
0.69167
0.74186
0.74627
0.74055
1.01539
1.02886
1.01623
1.00618
1.00395
1.00686
imgRV
imgAL
imgAWO
isoRV
isoAL
isoAWO

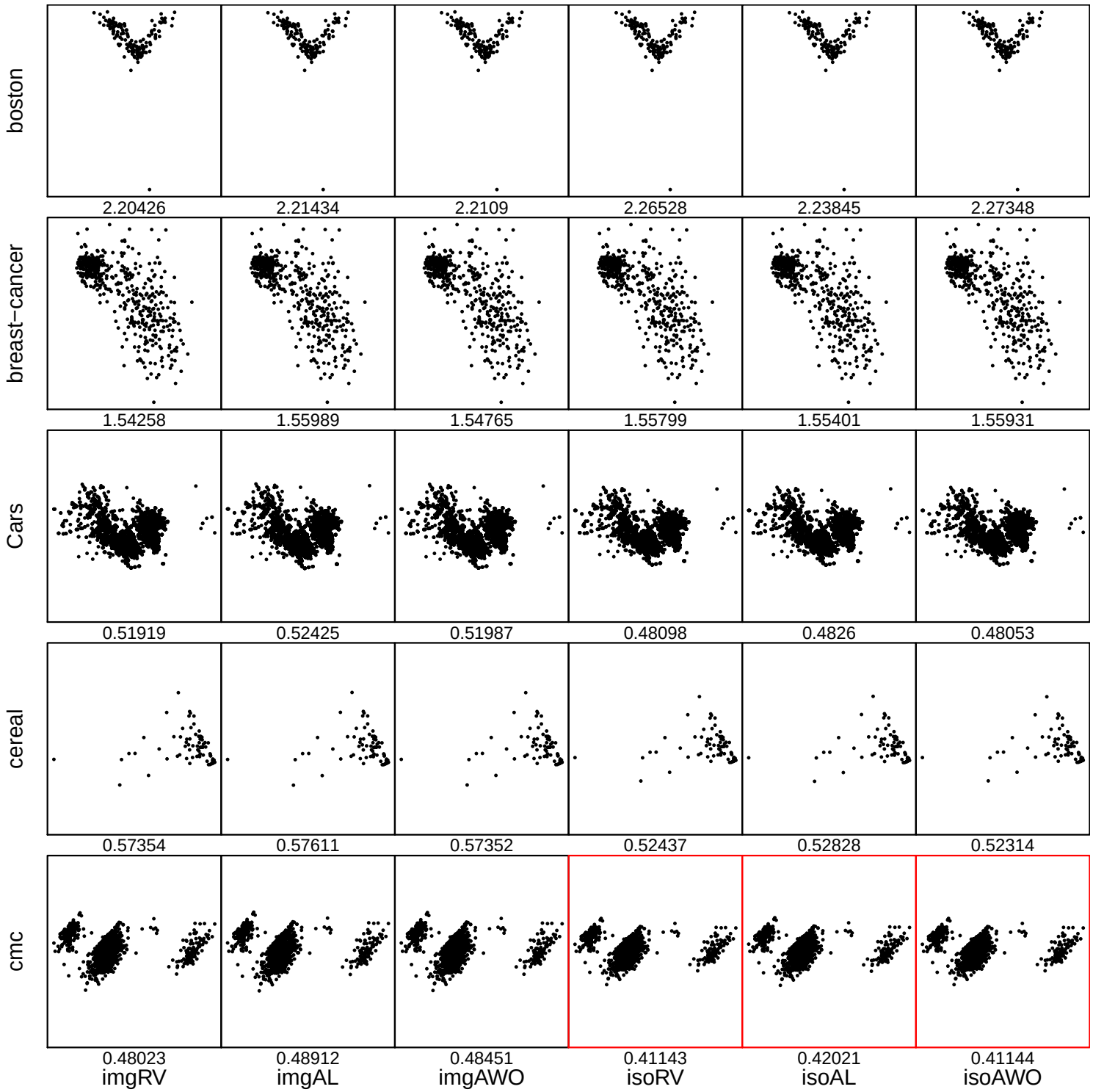
boston
breast−cancer
Cars
cereal
cmc
2.20426
2.21434
2.2109
2.26528
2.23845
2.27348
1.54258
1.55989
1.54765
1.55799
1.55401
1.55931
0.51919
0.52425
0.51987
0.48098
0.4826
0.48053
0.57354
0.57611
0.57352
0.52437
0.52828
0.52314
0.48023
0.48912
0.48451
0.41143
0.42021
0.41144
imgRV
imgAL
imgAWO
isoRV
isoAL
isoAWO

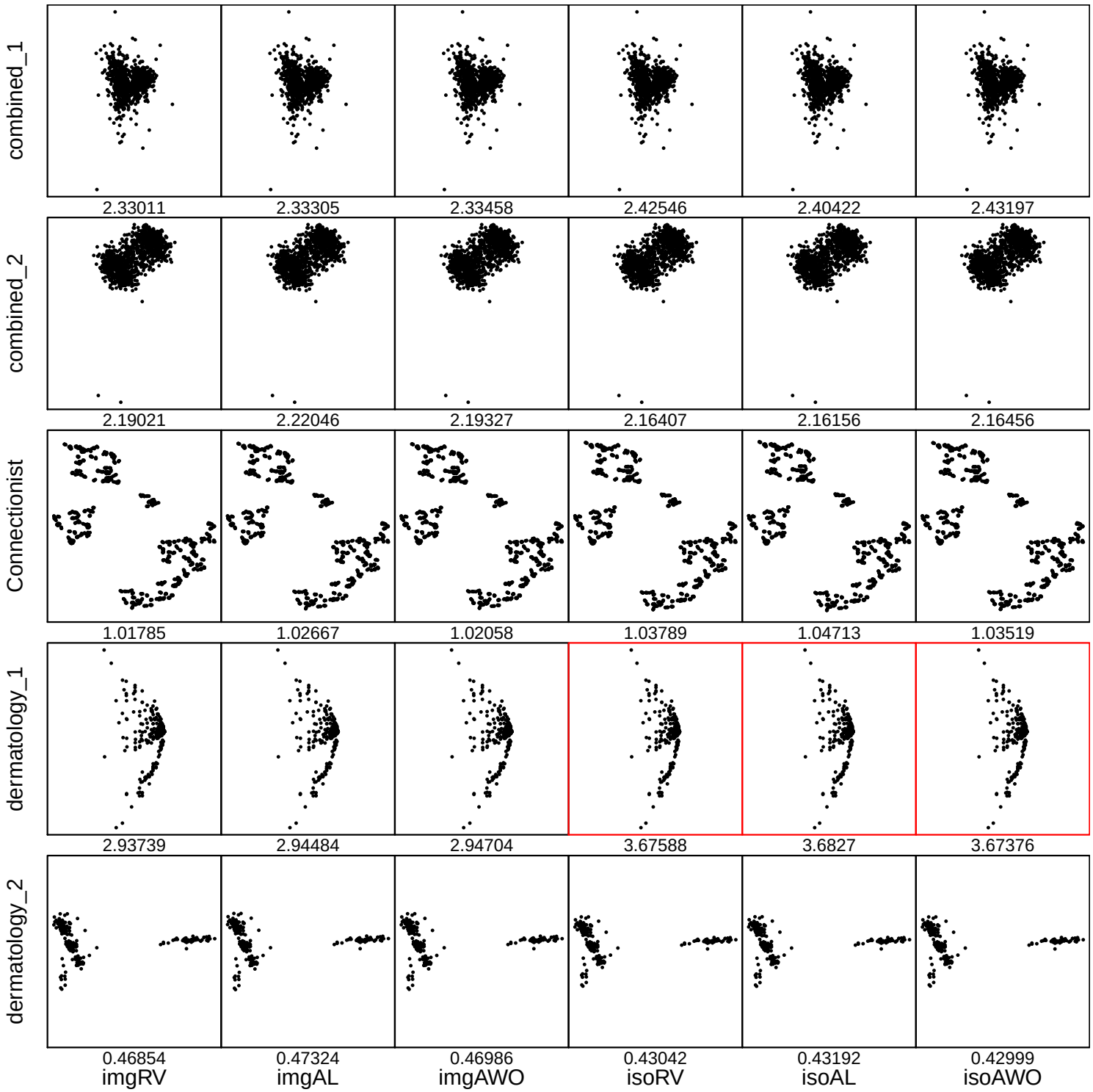
combined_1
2.33011
2.33305
2.33458
2.42546
2.40422
2.43197
combined_2
2.19021
2.22046
2.19327
2.16407
2.16156
2.16456
Connectionist
1.01785
1.02667
1.02058
1.03789
1.04713
1.03519
dermatology_1
2.93739
2.94484
2.94704
3.67588
3.6827
3.67376
dermatology_2
0.46854
0.47324
0.46986
0.43042
0.43192
0.42999
imgRV
imgAL
imgAWO
isoRV
isoAL
isoAWO

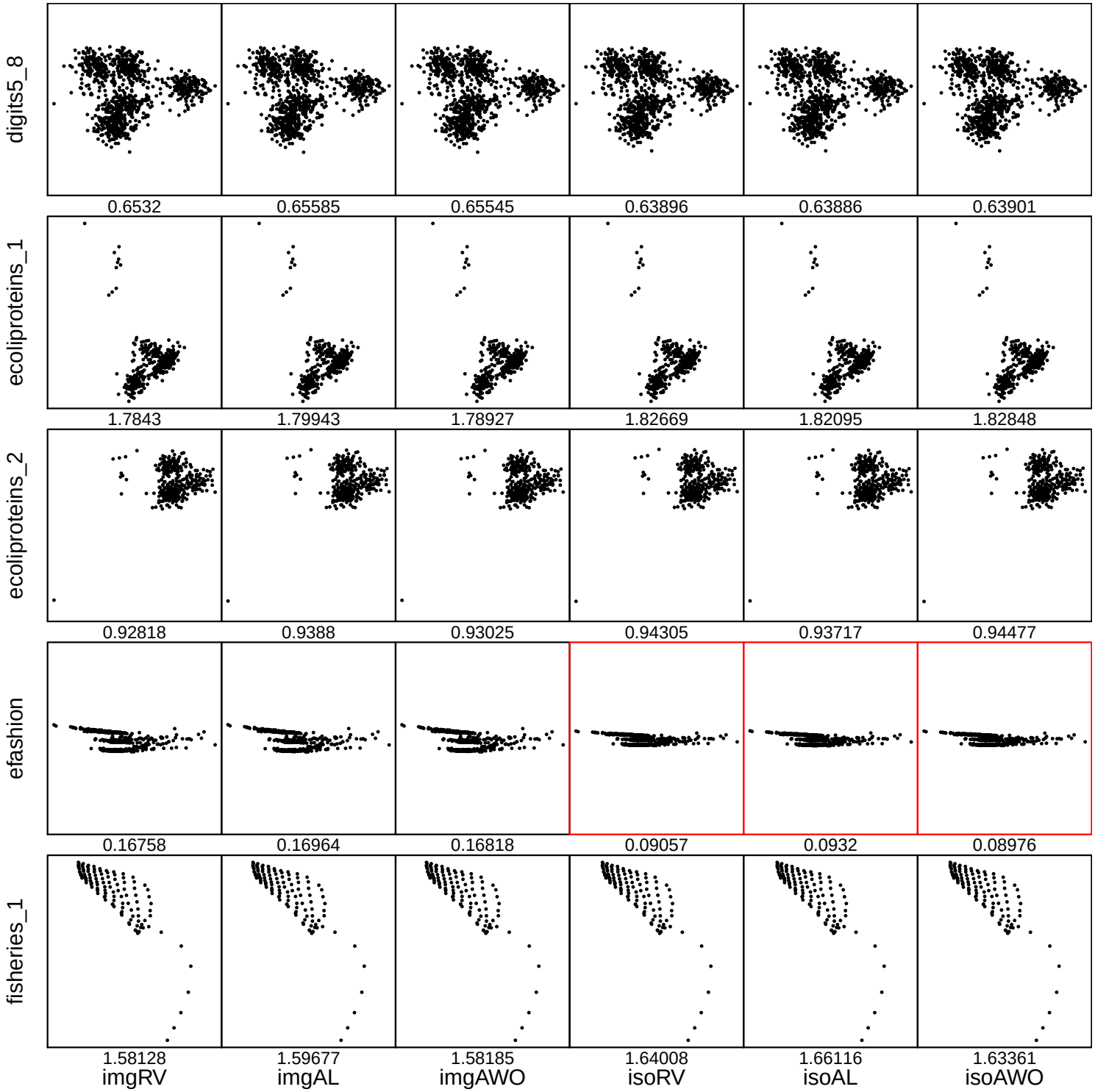
digits5_8
0.6532
0.65585
0.65545
0.63896
0.63886
0.63901
ecoliproteins_1
1.7843
1.79943
1.78927
1.82669
1.82095
1.82848
ecoliproteins_2
0.92818
0.9388
0.93025
0.94305
0.93717
0.94477
efashion
0.16758
0.16964
0.16818
0.09057
0.0932
0.08976
fisheries_1
1.58128
1.59677
1.58185
1.64008
1.66116
1.63361
imgRV
imgAL
imgAWO
isoRV
isoAL
isoAWO

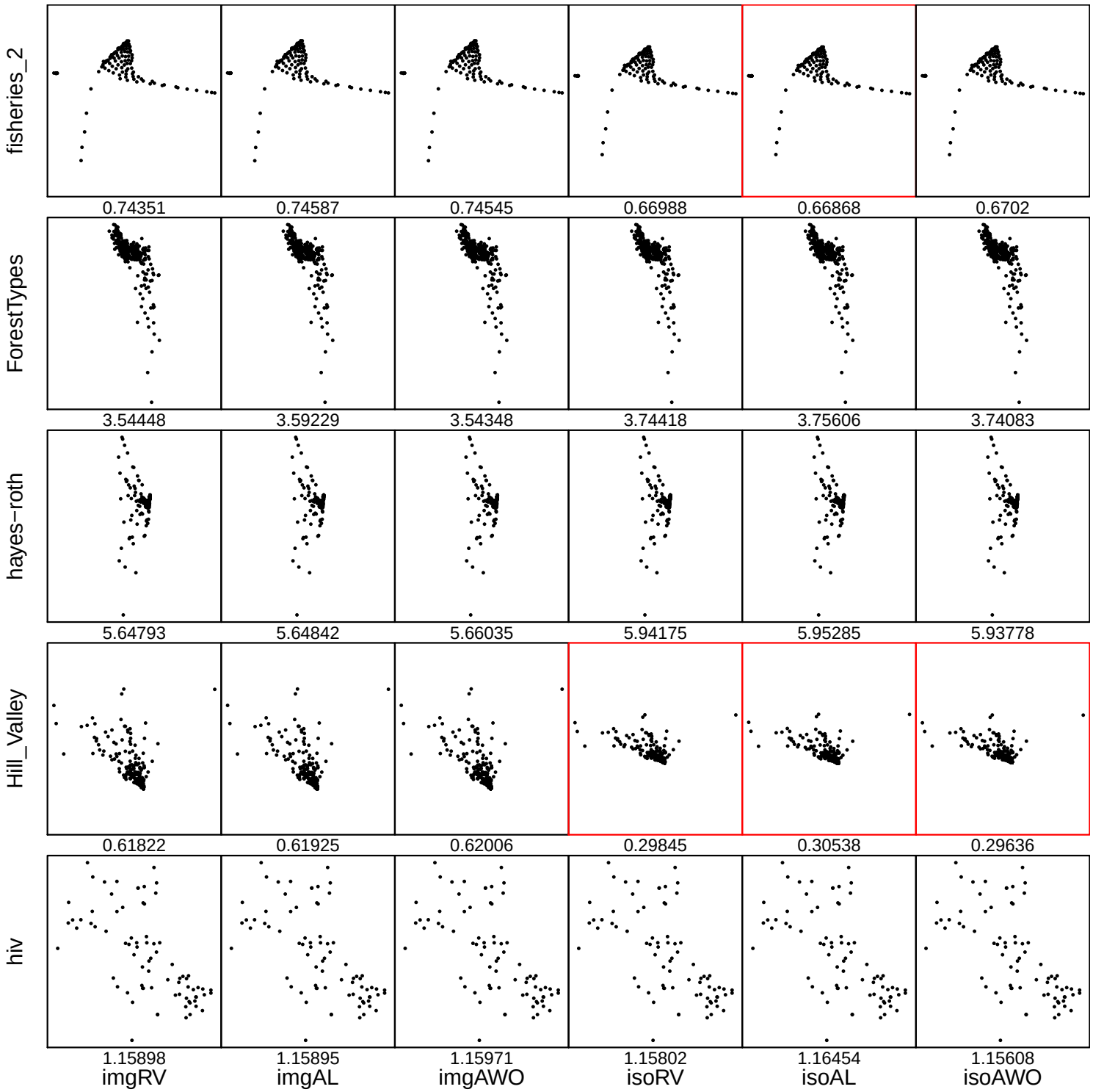
fisheries_2
0.74351
0.74587
0.74545
0.66988
0.66868
0.6702
ForestTypes
3.54448
3.59229
3.54348
3.74418
3.75606
3.74083
hayes−roth
5.64793
5.64842
5.66035
5.94175
5.95285
5.93778
Hill_Valley
0.61822
0.61925
0.62006
0.29845
0.30538
0.29636
hiv
1.15898
1.15895
1.15971
1.15802
1.16454
1.15608
imgRV
imgAL
imgAWO
isoRV
isoAL
isoAWO

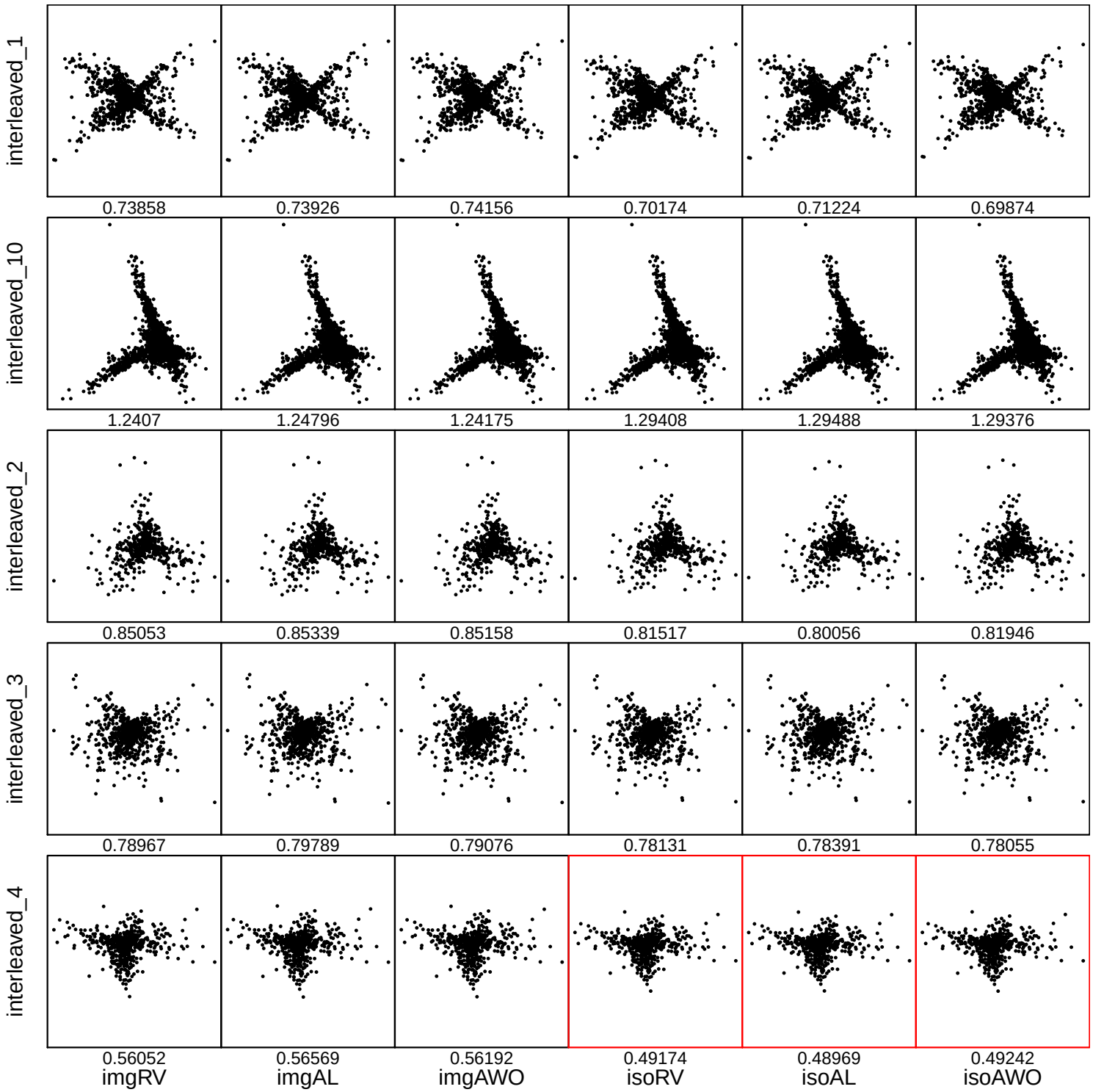
interleaved_1
0.73858
0.73926
0.74156
0.70174
0.71224
0.69874
interleaved_10
1.2407
1.24796
1.24175
1.29408
1.29488
1.29376
interleaved_2
0.85053
0.85339
0.85158
0.81517
0.80056
0.81946
interleaved_3
0.78967
0.79789
0.79076
0.78131
0.78391
0.78055
interleaved_4
0.56052
0.56569
0.56192
0.49174
0.48969
0.49242
imgRV
imgAL
imgAWO
isoRV
isoAL
isoAWO

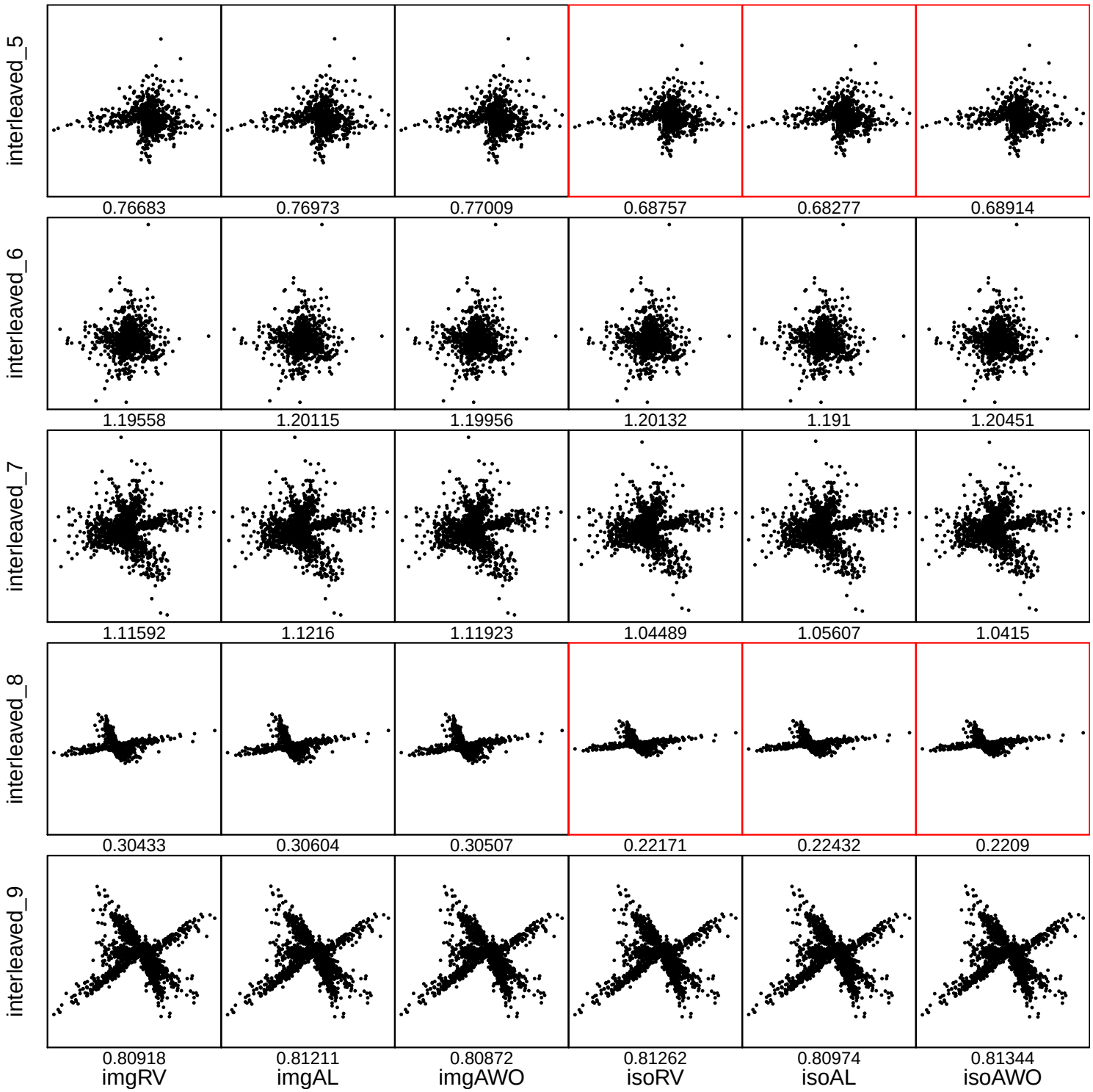
interleaved_5
0.76683
0.76973
0.77009
0.68757
0.68277
0.68914
interleaved_6
1.19558
1.20115
1.19956
1.20132
1.191
1.20451
interleaved_7
1.11592
1.1216
1.11923
1.04489
1.05607
1.0415
interleaved_8
0.30433
0.30604
0.30507
0.22171
0.22432
0.2209
interleaved_9
0.80918
0.81211
0.80872
0.81262
0.80974
0.81344
imgRV
imgAL
imgAWO
isoRV
isoAL
isoAWO

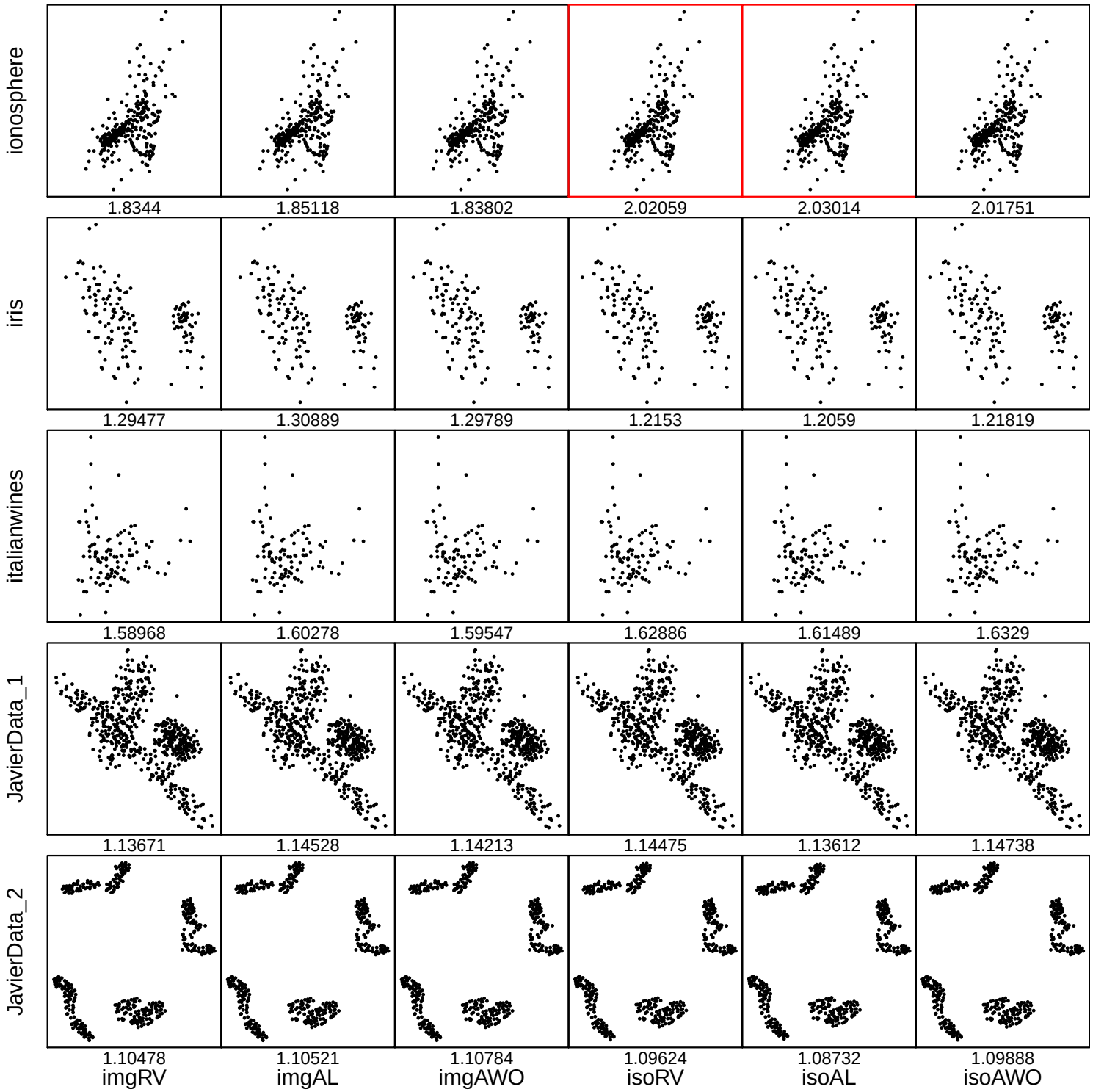
ionosphere
1.8344
1.85118
1.83802
2.02059
2.03014
2.01751
iris
1.29477
1.30889
1.29789
1.2153
1.2059
1.21819
italianwines
1.58968
1.60278
1.59547
1.62886
1.61489
1.6329
JavierData_1
1.13671
1.14528
1.14213
1.14475
1.13612
1.14738
JavierData_2
1.10478
1.10521
1.10784
1.09624
1.08732
1.09888
imgRV
imgAL
imgAWO
isoRV
isoAL
isoAWO

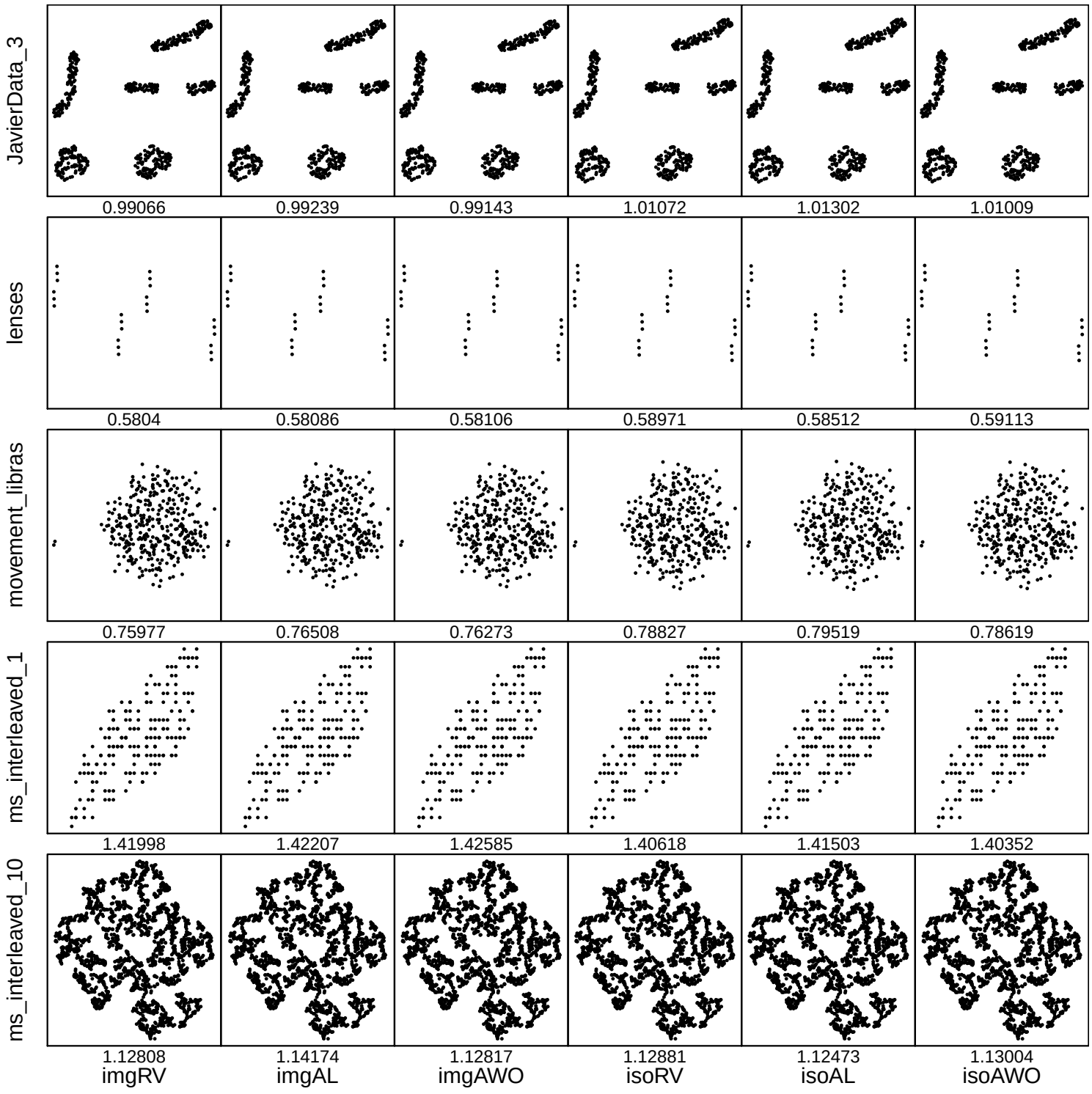
JavierData_3
0.99066
0.99239
0.99143
1.01072
1.01302
1.01009
lenses
0.5804
0.58086
0.58106
0.58971
0.58512
0.59113
movement_libras
0.75977
0.76508
0.76273
0.78827
0.79519
0.78619
ms_interleaved_1
1.41998
1.42207
1.42585
1.40618
1.41503
1.40352
ms_interleaved_10
1.12808
1.14174
1.12817
1.12881
1.12473
1.13004
imgRV
imgAL
imgAWO
isoRV
isoAL
isoAWO

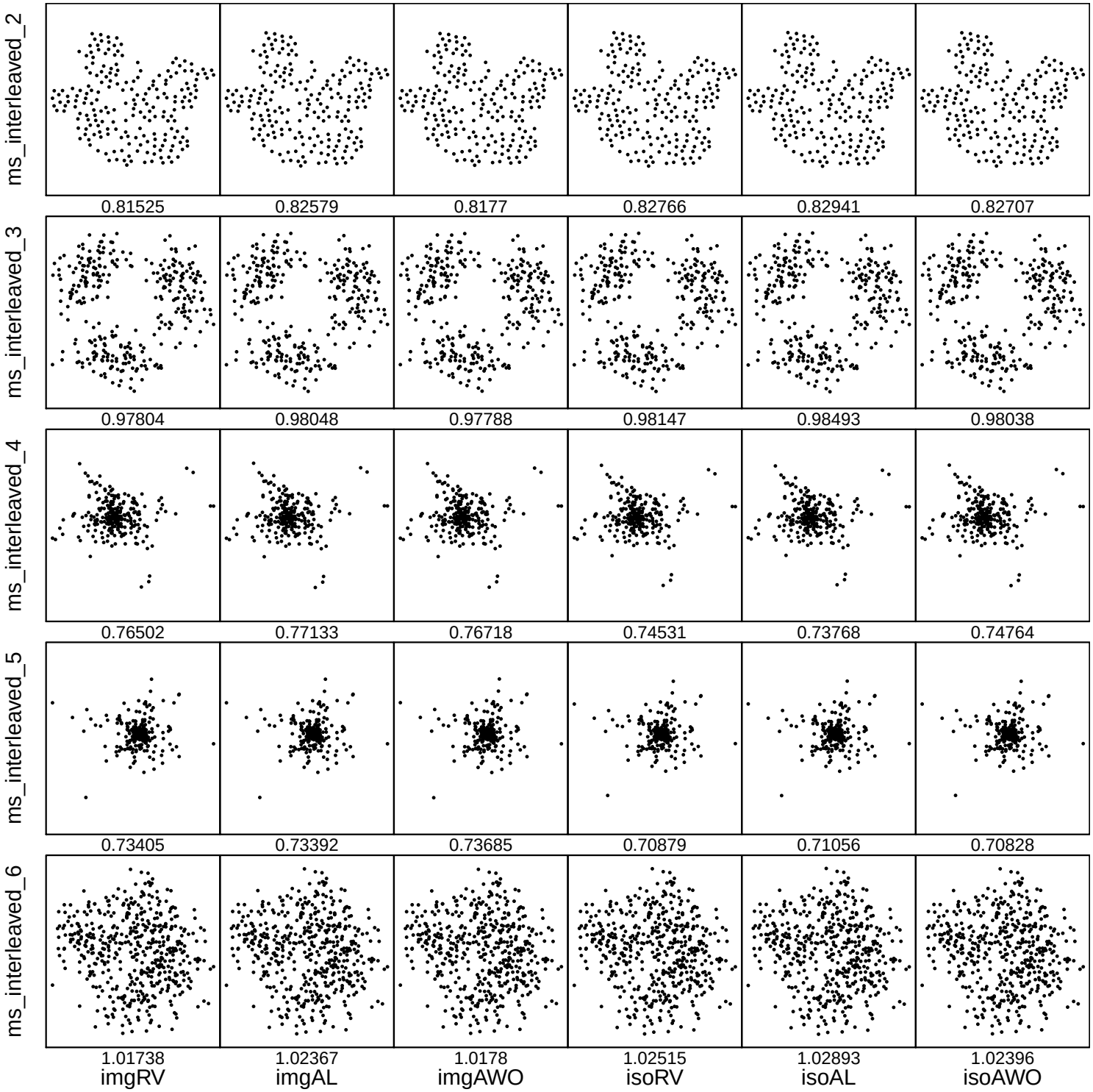
ms_interleaved_2
ms_interleaved_3
ms_interleaved_4
ms_interleaved_5
ms_interleaved_6
0.81525
0.82579
0.8177
0.82766
0.82941
0.82707
0.97804
0.98048
0.97788
0.98147
0.98493
0.98038
0.76502
0.77133
0.76718
0.74531
0.73768
0.74764
0.73405
0.73392
0.73685
0.70879
0.71056
0.70828
1.01738
1.02367
1.0178
1.02515
1.02893
1.02396
imgRV
imgAL
imgAWO
isoRV
isoAL
isoAWO

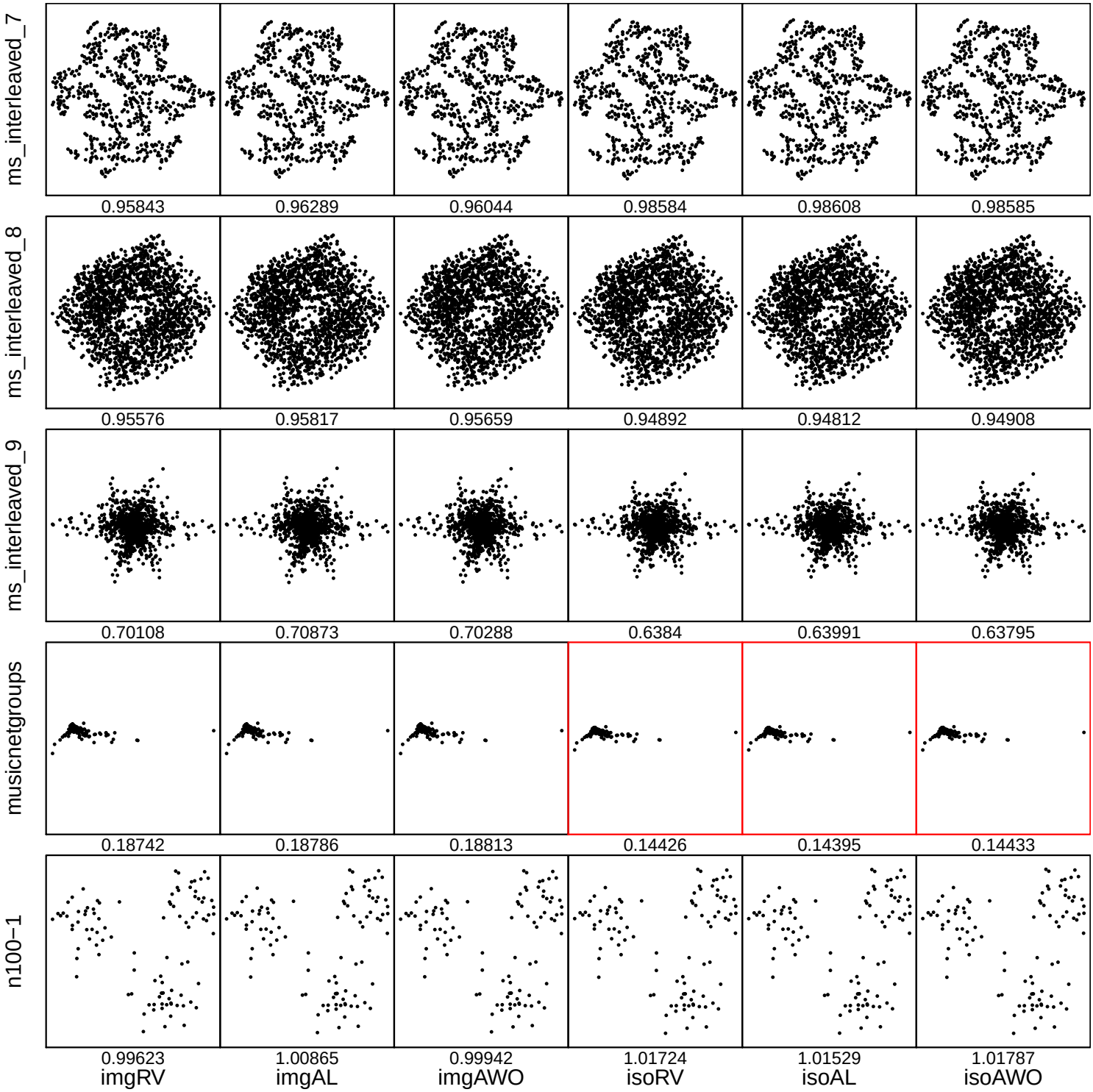
ms_interleaved_7
0.95843
0.96289
0.96044
0.98584
0.98608
0.98585
ms_interleaved_8
0.95576
0.95817
0.95659
0.94892
0.94812
0.94908
ms_interleaved_9
0.70108
0.70873
0.70288
0.6384
0.63991
0.63795
musicnetgroups
0.18742
0.18786
0.18813
0.14426
0.14395
0.14433
n100−1
0.99623
imgRV
1.00865
imgAL
0.99942
imgAWO
1.01724
isoRV
1.01529
isoAL
1.01787
isoAWO

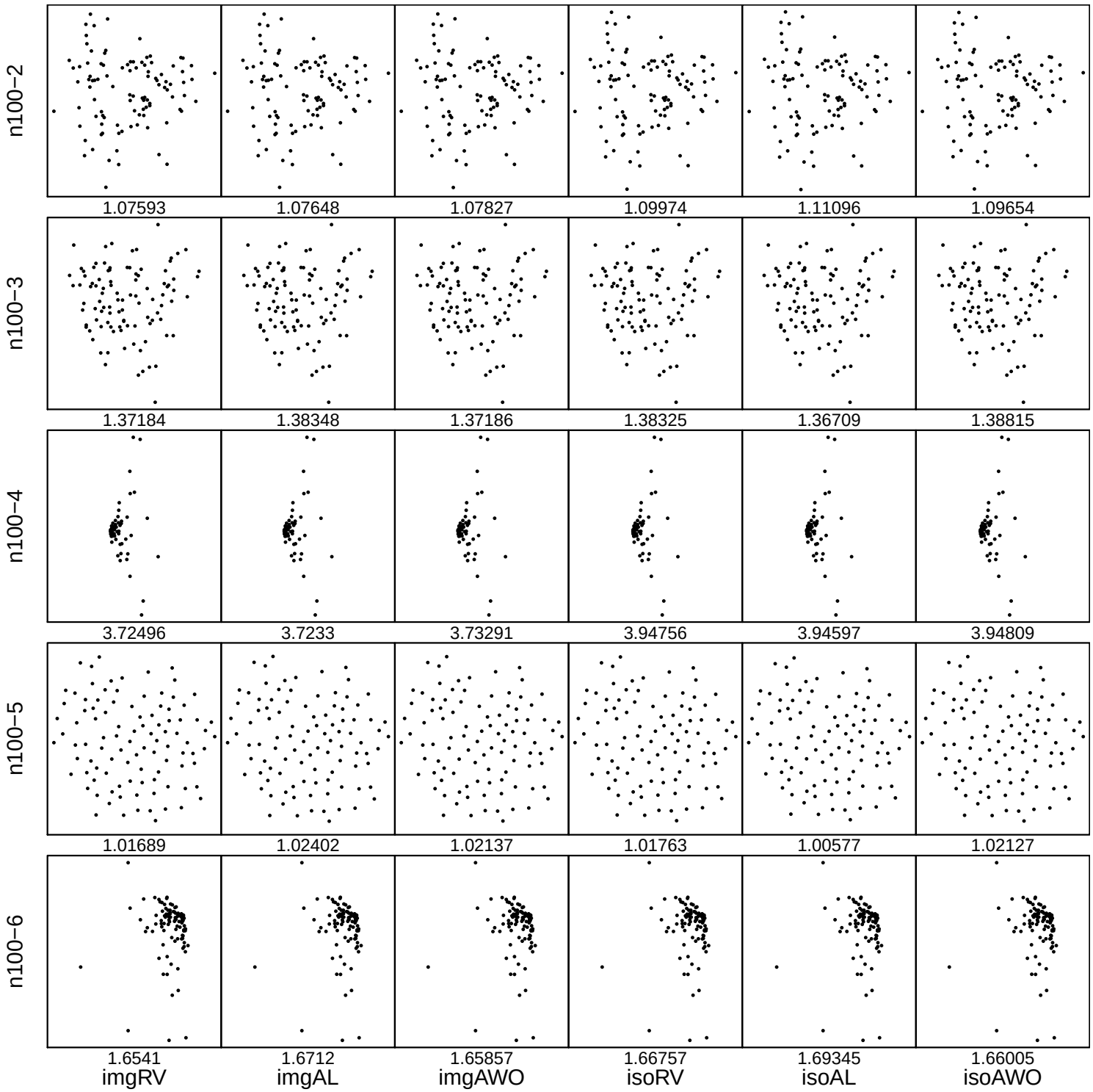
n100−2
n100−3
n100−4
n100−5
n100−6
1.07593
1.07648
1.07827
1.09974
1.11096
1.09654
1.37184
1.38348
1.37186
1.38325
1.36709
1.38815
3.72496
3.7233
3.73291
3.94756
3.94597
3.94809
1.01689
1.02402
1.02137
1.01763
1.00577
1.02127
1.6541
1.6712
1.65857
1.66757
1.69345
1.66005
imgRV
imgAL
imgAWO
isoRV
isoAL
isoAWO

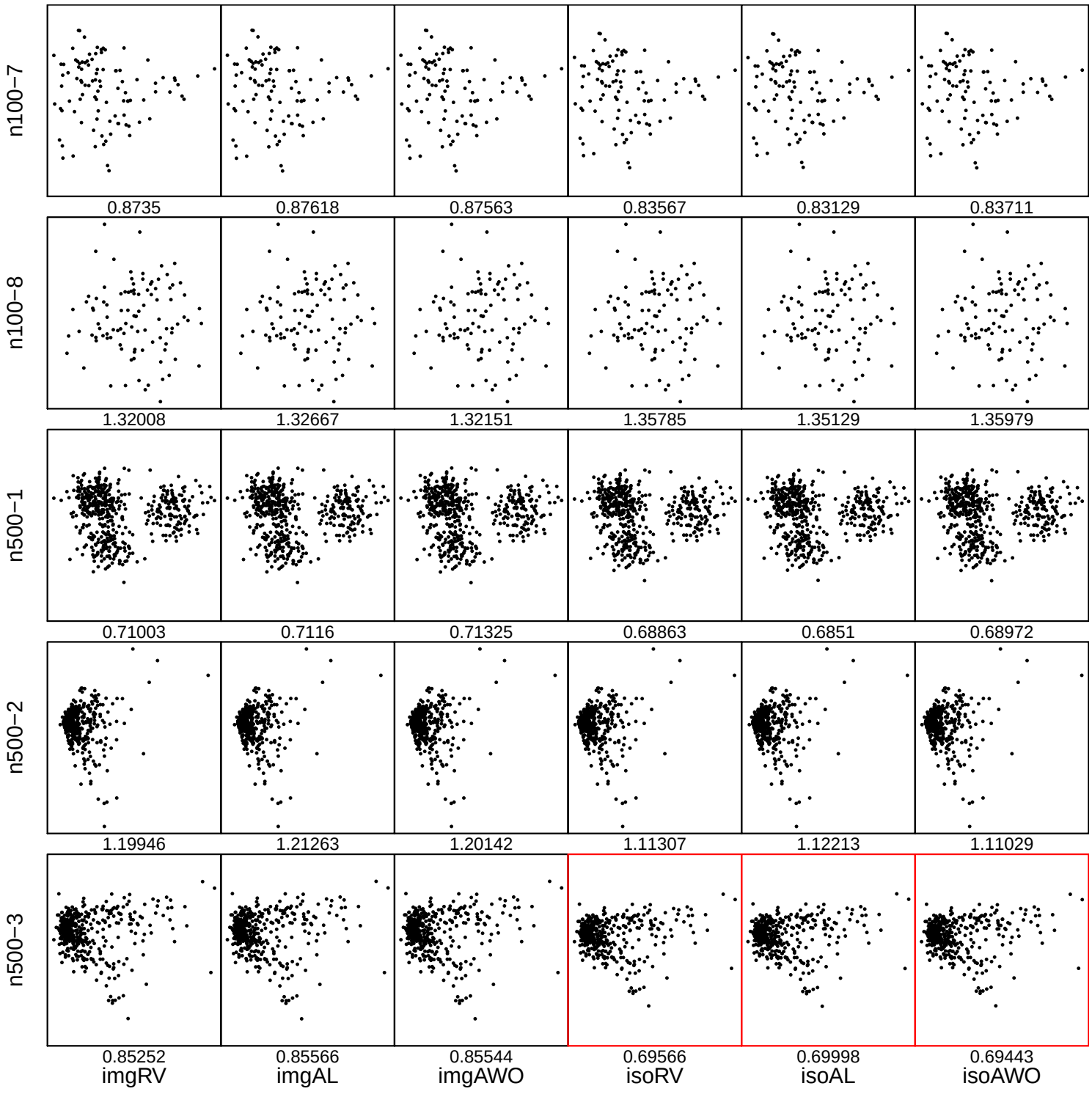
n100−7
0.8735
0.87618
0.87563
0.83567
0.83129
0.83711
n100−8
1.32008
1.32667
1.32151
1.35785
1.35129
1.35979
n500−1
0.71003
0.7116
0.71325
0.68863
0.6851
0.68972
n500−2
1.19946
1.21263
1.20142
1.11307
1.12213
1.11029
n500−3
0.85252
0.85566
0.85544
0.69566
0.69998
0.69443
imgRV
imgAL
imgAWO
isoRV
isoAL
isoAWO

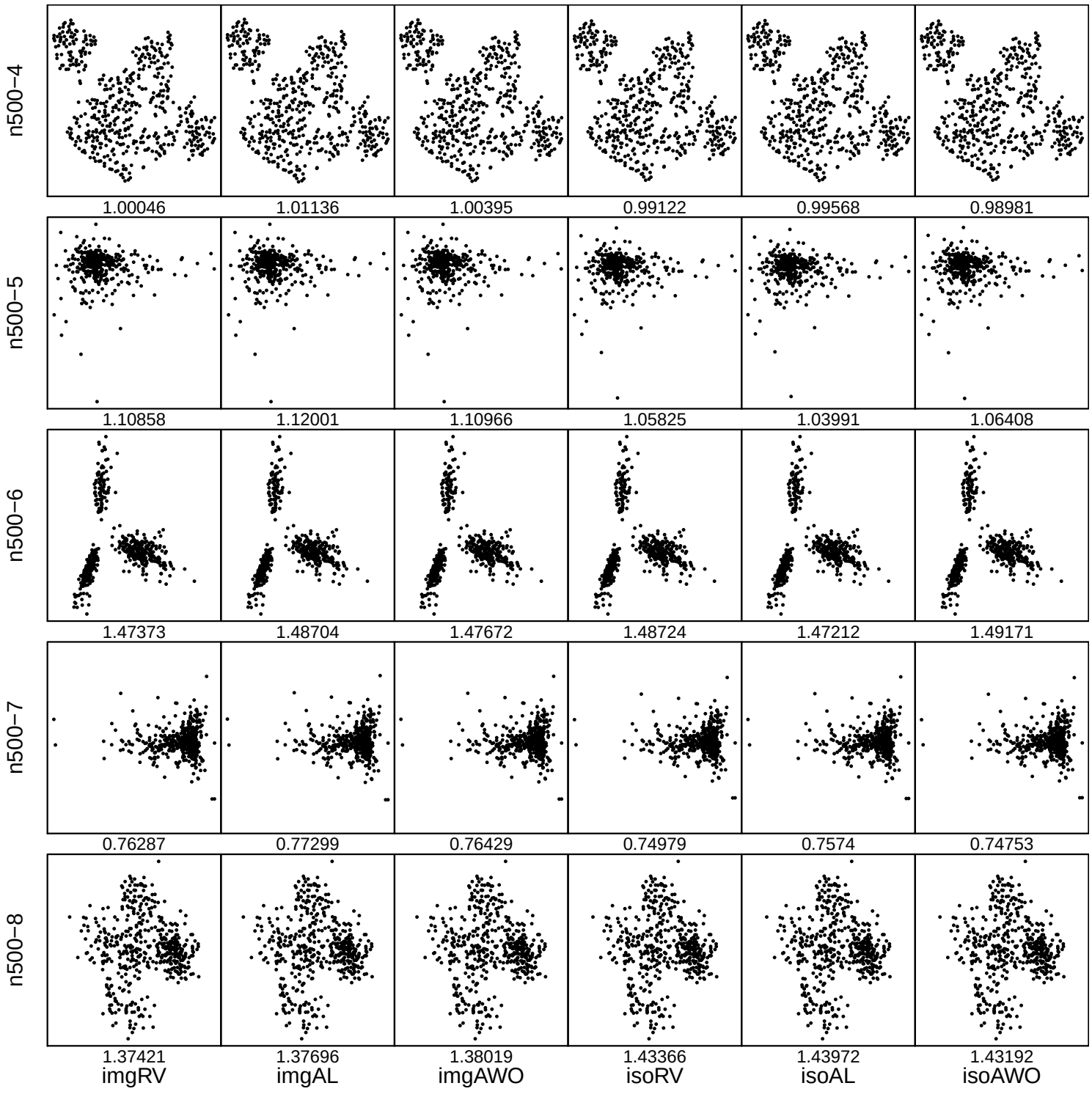
n500−4
n500−5
n500−6
n500−7
n500−8
1.00046
1.01136
1.00395
0.99122
0.99568
0.98981
1.10858
1.12001
1.10966
1.05825
1.03991
1.06408
1.47373
1.48704
1.47672
1.48724
1.47212
1.49171
0.76287
0.77299
0.76429
0.74979
0.7574
0.74753
1.37421
1.37696
1.38019
1.43366
1.43972
1.43192
imgRV
imgAL
imgAWO
isoRV
isoAL
isoAWO

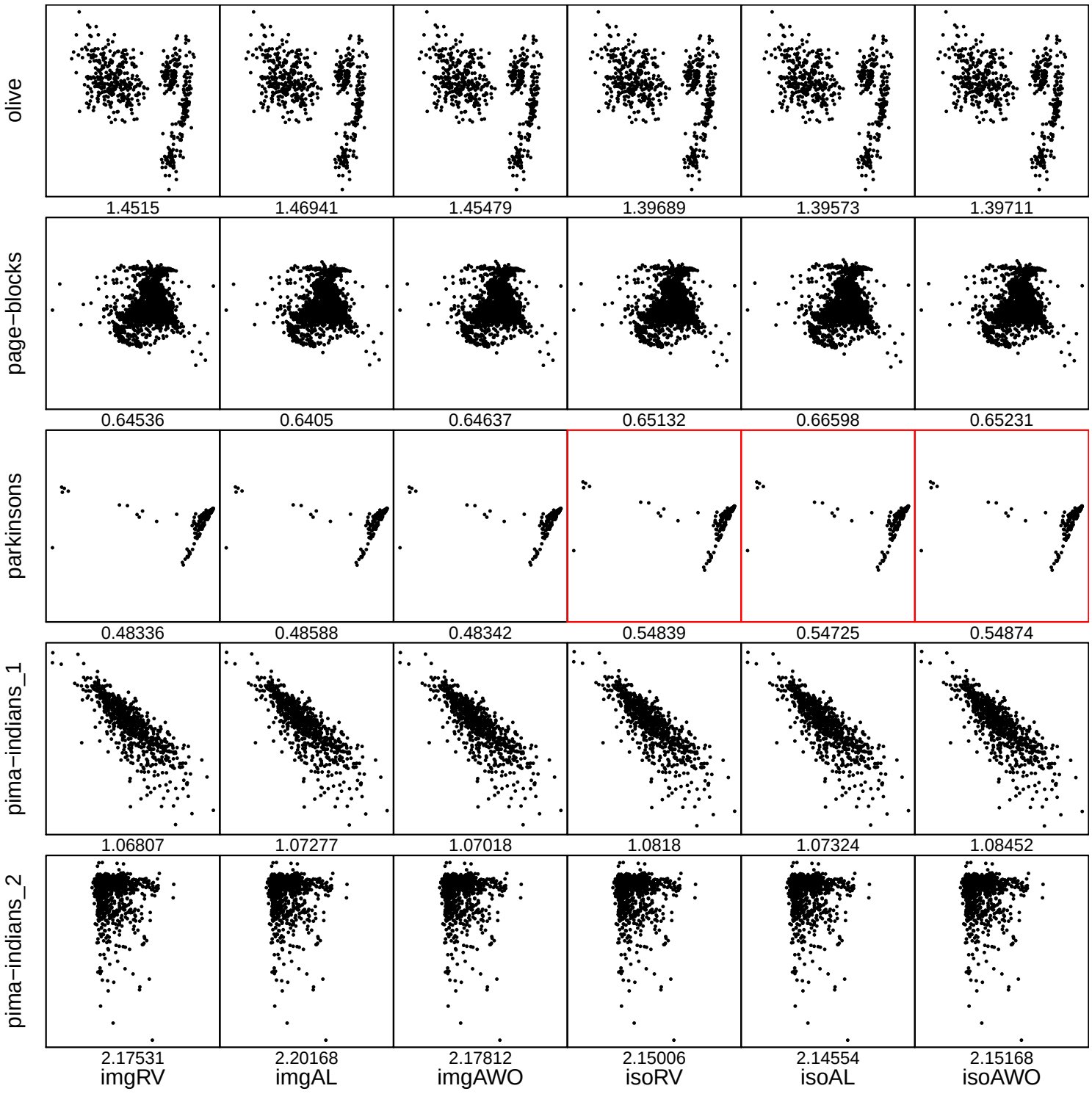
olive
1.4515
1.46941
1.45479
1.39689
1.39573
1.39711
page−blocks
0.64536
0.6405
0.64637
0.65132
0.66598
0.65231
parkinsons
0.48336
0.48588
0.48342
0.54839
0.54725
0.54874
pima−indians_1
1.06807
1.07277
1.07018
1.0818
1.07324
1.08452
pima−indians_2
2.17531
imgRV
2.20168
imgAL
2.17812
imgAWO
2.15006
isoRV
2.14554
isoAL
2.15168
isoAWO

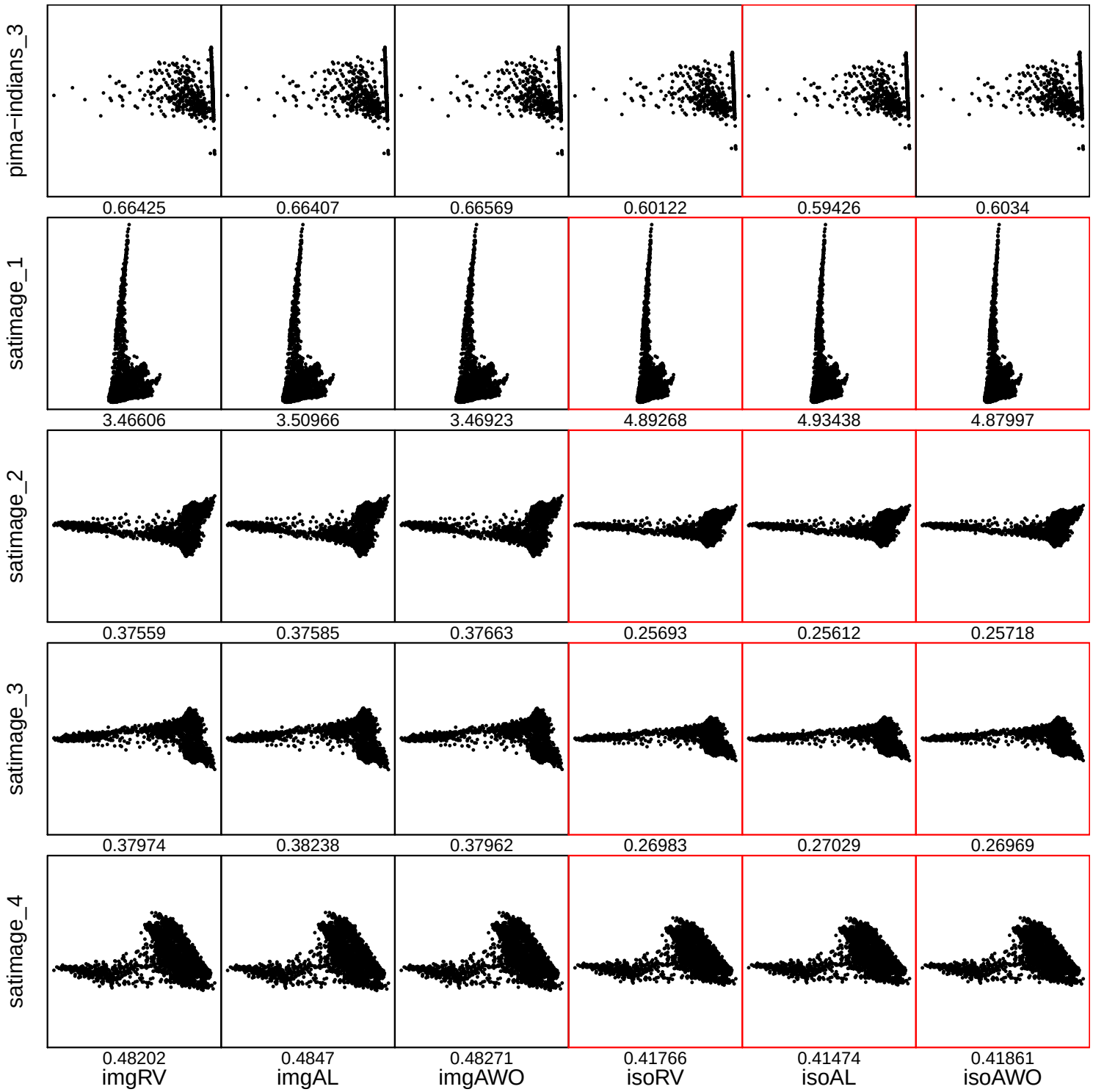
pima−indians_3
0.66425
0.66407
0.66569
0.60122
0.59426
0.6034
satimage_1
3.46606
3.50966
3.46923
4.89268
4.93438
4.87997
satimage_2
0.37559
0.37585
0.37663
0.25693
0.25612
0.25718
satimage_3
0.37974
0.38238
0.37962
0.26983
0.27029
0.26969
satimage_4
0.48202
0.4847
0.48271
0.41766
0.41474
0.41861
imgRV
imgAL
imgAWO
isoRV
isoAL
isoAWO

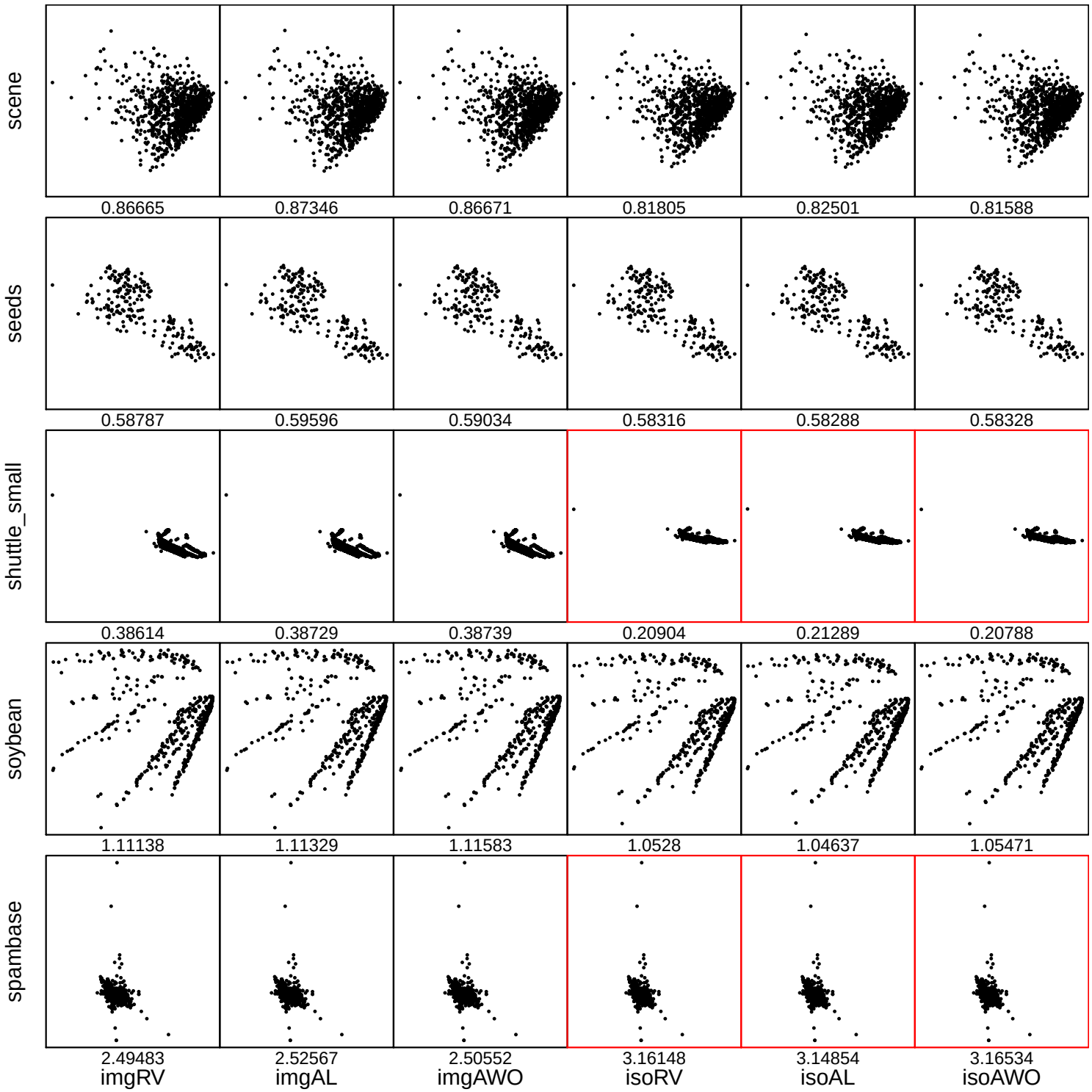
scene
seeds
shuttle_small
soybean
spambase
0.86665
0.87346
0.86671
0.81805
0.82501
0.81588
0.58787
0.59596
0.59034
0.58316
0.58288
0.58328
0.38614
0.38729
0.38739
0.20904
0.21289
0.20788
1.11138
1.11329
1.11583
1.0528
1.04637
1.05471
2.49483
2.52567
2.50552
3.16148
3.14854
3.16534
imgRV
imgAL
imgAWO
isoRV
isoAL
isoAWO

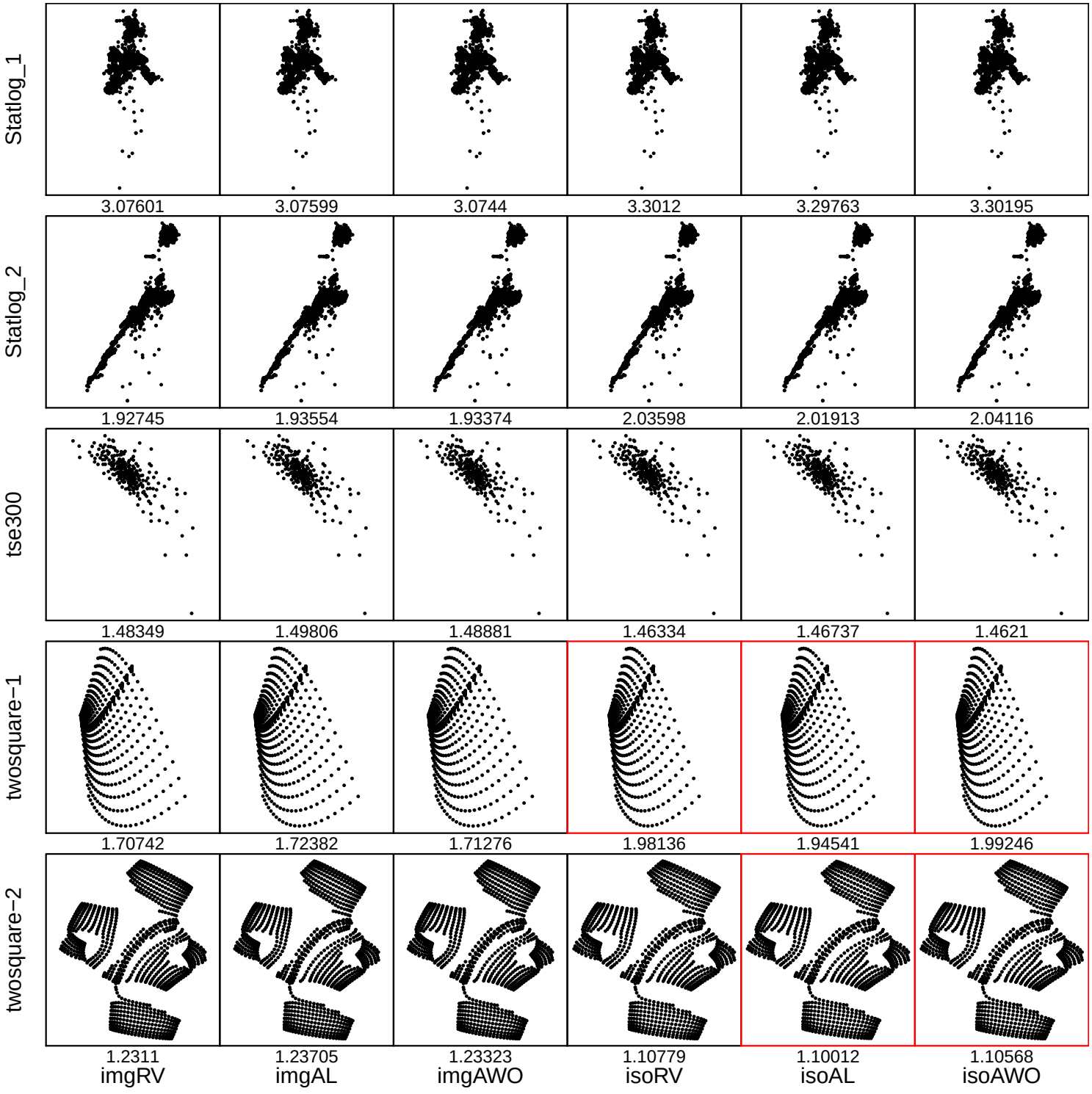
Statlog_1
3.07601
3.07599
3.0744
3.3012
3.29763
3.30195
Statlog_2
1.92745
1.93554
1.93374
2.03598
2.01913
2.04116
tse300
1.48349
1.49806
1.48881
1.46334
1.46737
1.4621
twosquare−1
1.70742
1.72382
1.71276
1.98136
1.94541
1.99246
twosquare−2
1.2311
1.23705
1.23323
1.10779
1.10012
1.10568
imgRV
imgAL
imgAWO
isoRV
isoAL
isoAWO

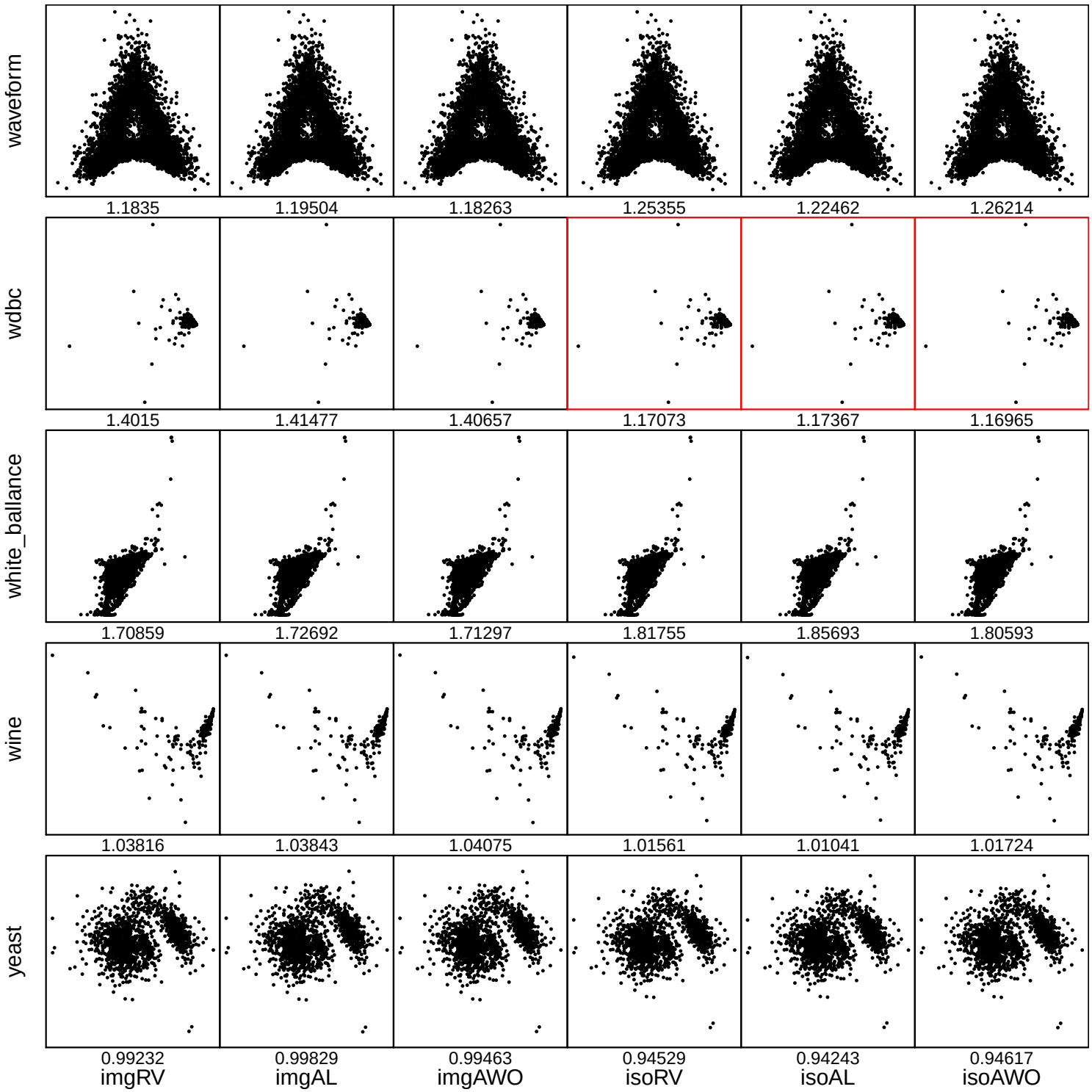
waveform
1.1835
1.19504
1.18263
1.25355
1.22462
1.26214
wdbc
1.4015
1.41477
1.40657
1.17073
1.17367
1.16965
white_ballance
1.70859
1.72692
1.71297
1.81755
1.85693
1.80593
wine
1.03816
1.03843
1.04075
1.01561
1.01041
1.01724
yeast
0.99232
0.99829
0.99463
0.94529
0.94243
0.94617
imgRV
imgAL
imgAWO
isoRV
isoAL
isoAWO

APPENDIX B: COMPREHENSIVE COMPARISON OF SIX METHODS WITH 500 ISOVALUES

In this appendix, we present the detailed results with all 100 datasets from [4, 9] for comprehensive comparison of the six methods described in Section 2. Note that the number of isovalues $m = 500$. Moreover, there are no results whose deviations with isoRV (with $m = 1000$) are larger than 10%.

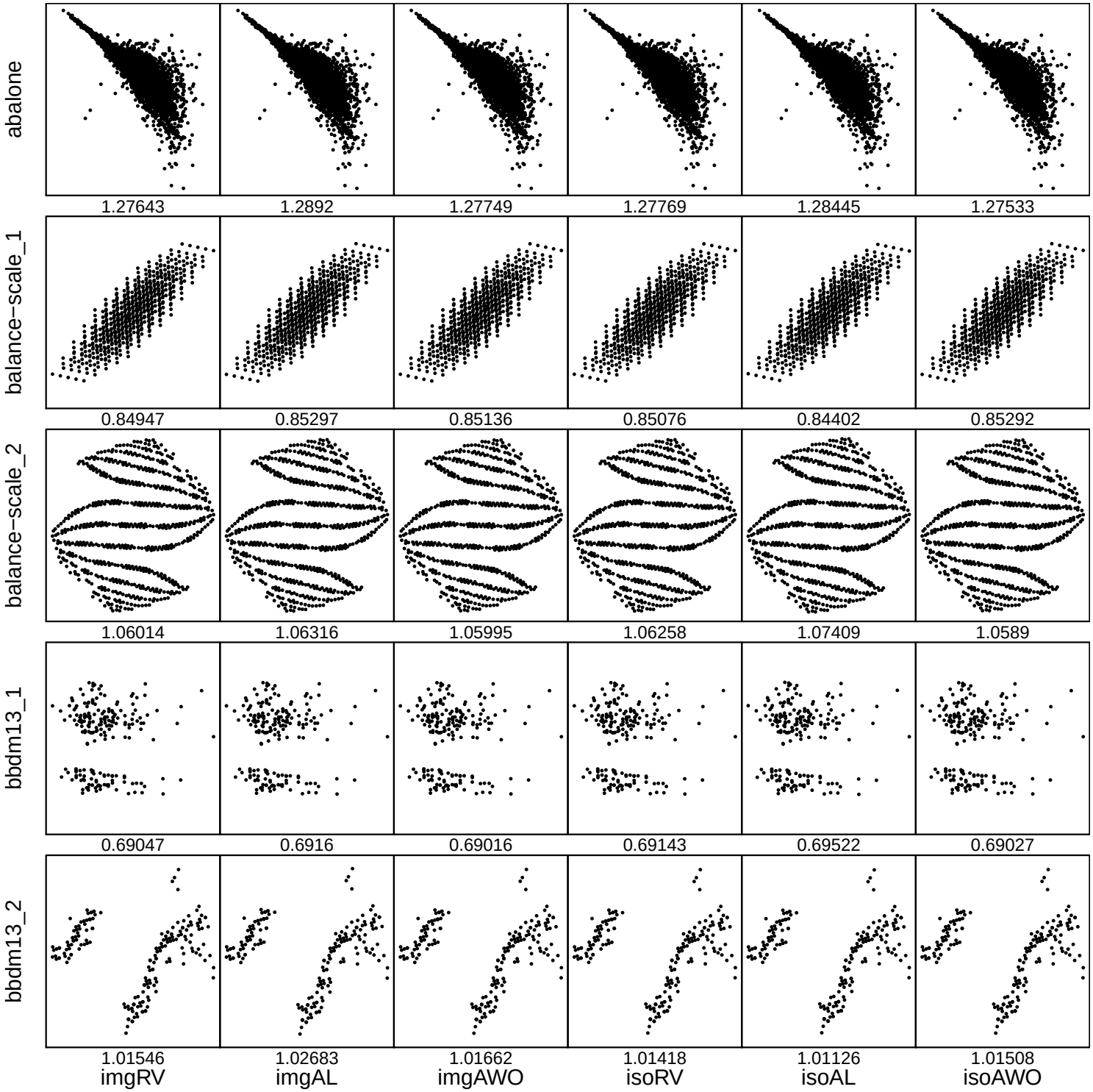
abalone
balance−scale_1
balance−scale_2
bbdm13_1
bbdm13_2
1.27643
1.2892
1.27749
1.27769
1.28445
1.27533
0.84947
0.85297
0.85136
0.85076
0.84402
0.85292
1.06014
1.06316
1.05995
1.06258
1.07409
1.0589
0.69047
0.6916
0.69016
0.69143
0.69522
0.69027
1.01546
1.02683
1.01662
1.01418
1.01126
1.01508
imgRV
imgAL
imgAWO
isoRV
isoAL
isoAWO

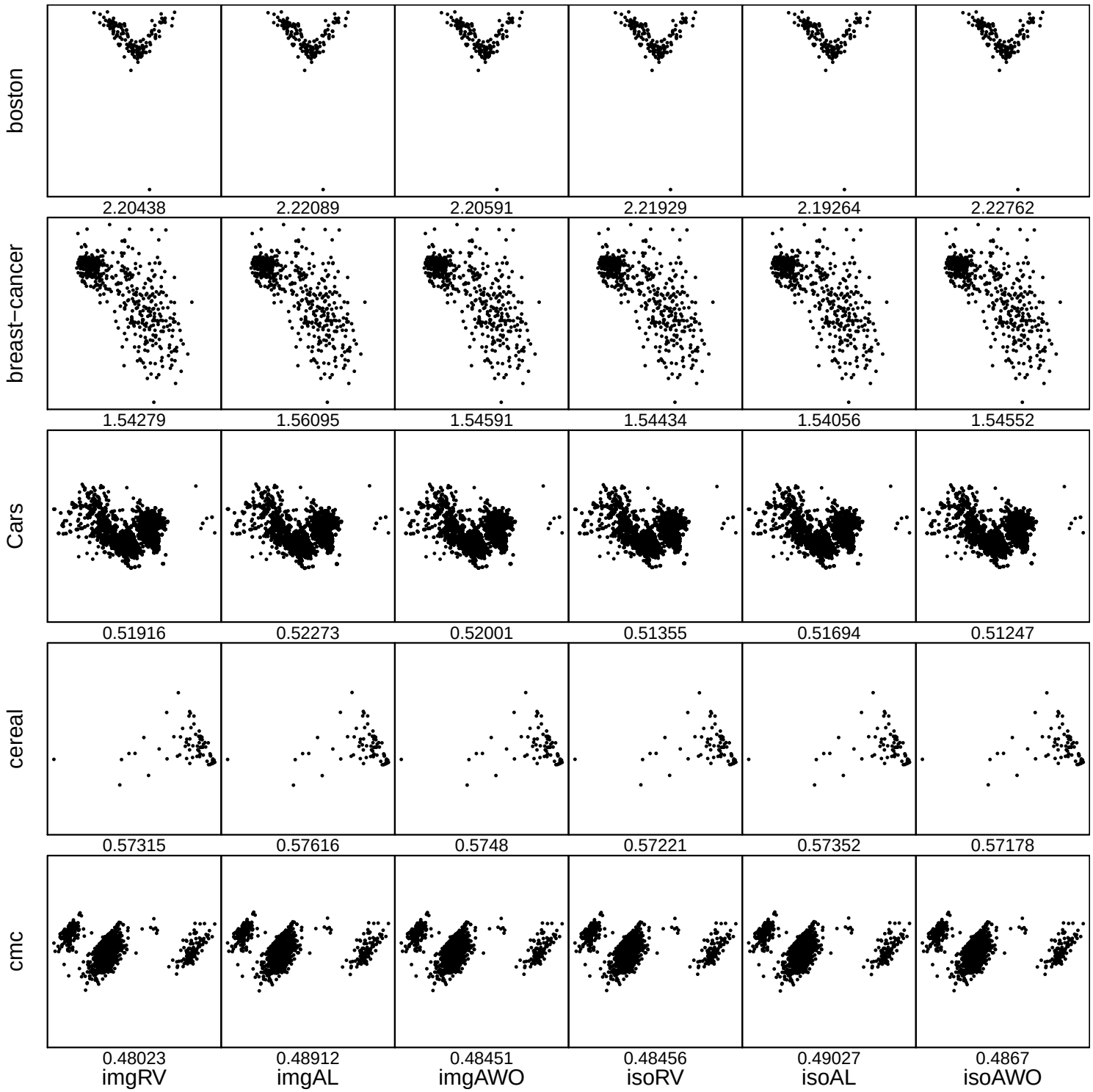
boston
breast−cancer
Cars
cereal
cmc
2.20438
2.22089
2.20591
2.21929
2.19264
2.22762
1.54279
1.56095
1.54591
1.54434
1.54056
1.54552
0.51916
0.52273
0.52001
0.51355
0.51694
0.51247
0.57315
0.57616
0.5748
0.57221
0.57352
0.57178
0.48023
0.48912
0.48451
0.48456
0.49027
0.4867
imgRV
imgAL
imgAWO
isoRV
isoAL
isoAWO

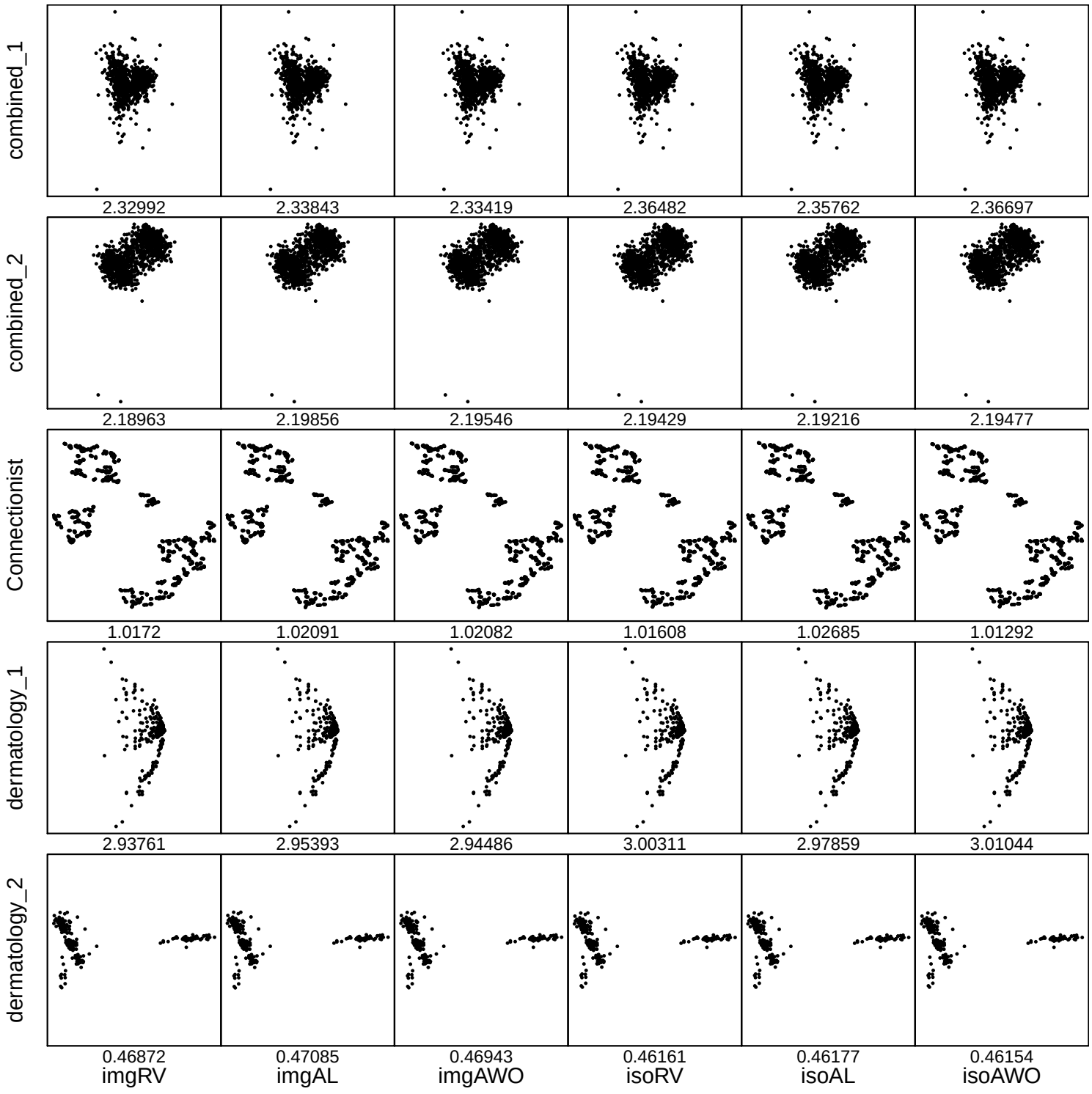
combined_1
2.32992
2.33843
2.33419
2.36482
2.35762
2.36697
combined_2
2.18963
2.19856
2.19546
2.19429
2.19216
2.19477
Connectionist
1.0172
1.02091
1.02082
1.01608
1.02685
1.01292
dermatology_1
2.93761
2.95393
2.94486
3.00311
2.97859
3.01044
dermatology_2
0.46872
0.47085
0.46943
0.46161
0.46177
0.46154
imgRV
imgAL
imgAWO
isoRV
isoAL
isoAWO

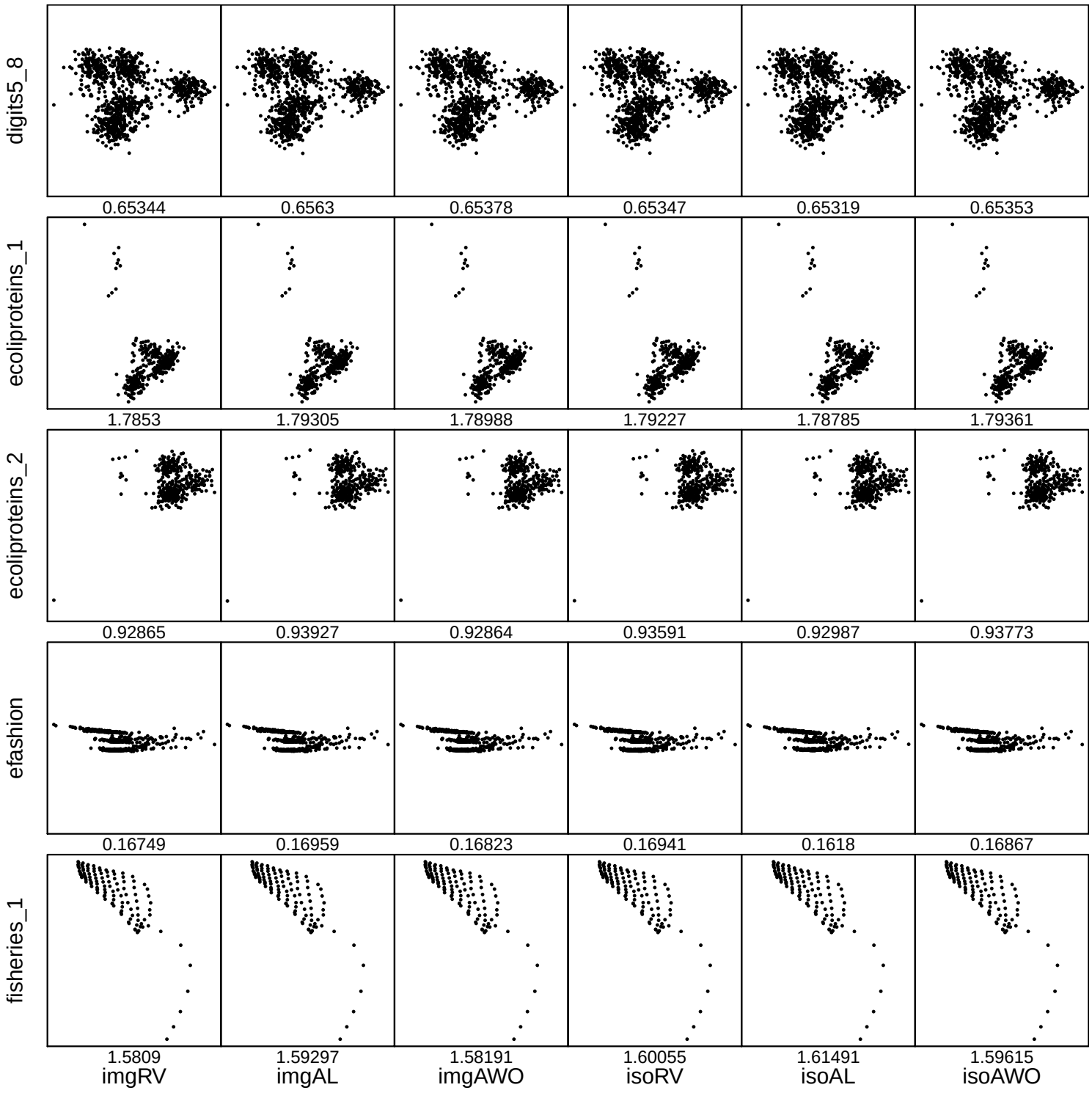
digits5_8
0.65344
0.6563
0.65378
0.65347
0.65319
0.65353
ecoliproteins_1
1.7853
1.79305
1.78988
1.79227
1.78785
1.79361
ecoliproteins_2
0.92865
0.93927
0.92864
0.93591
0.92987
0.93773
efashion
0.16749
0.16959
0.16823
0.16941
0.1618
0.16867
fisheries_1
1.5809
1.59297
1.58191
1.60055
1.61491
1.59615
imgRV
imgAL
imgAWO
isoRV
isoAL
isoAWO

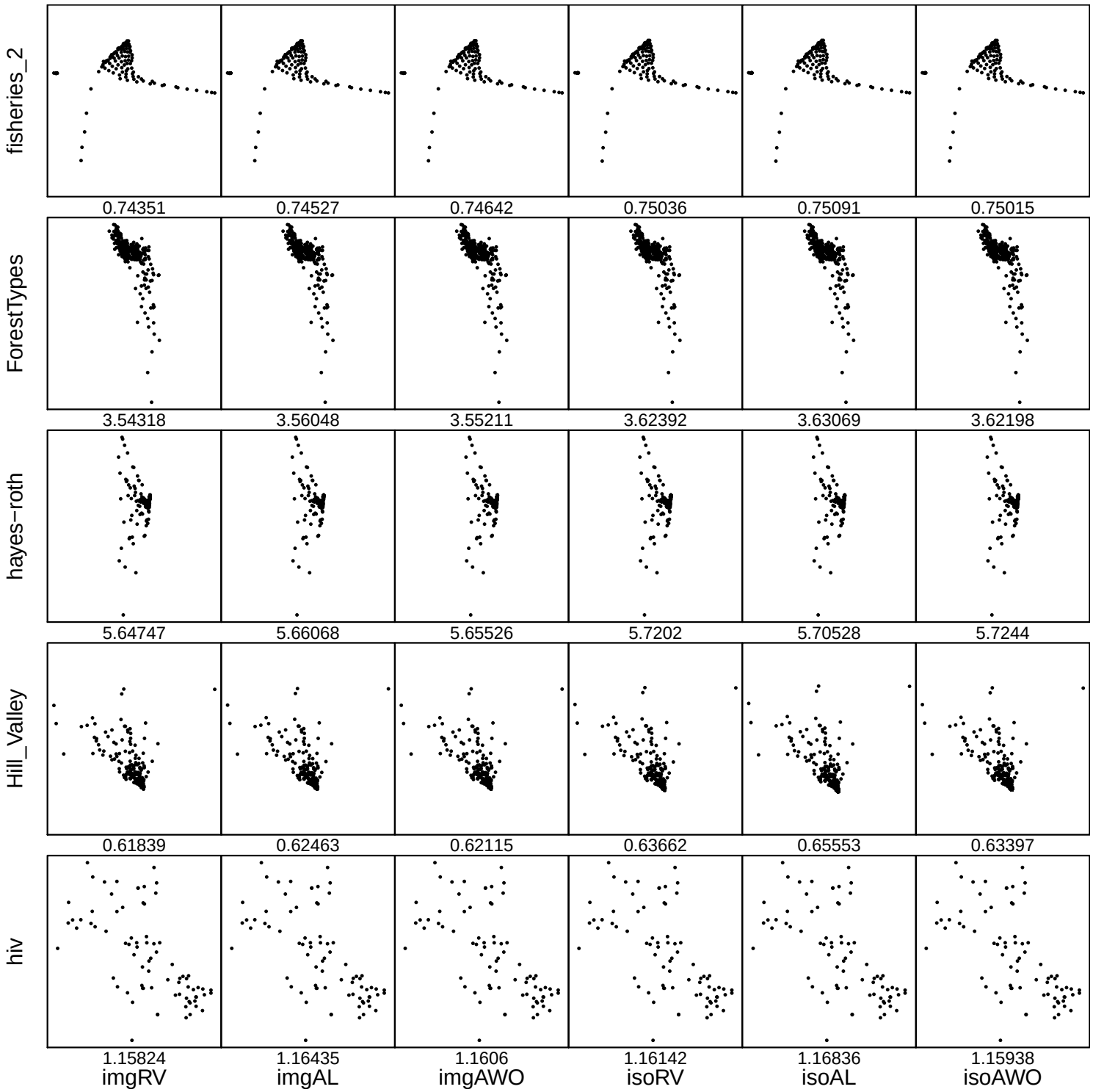
fisheries_2
0.74351
0.74527
0.74642
0.75036
0.75091
0.75015
ForestTypes
3.54318
3.56048
3.55211
3.62392
3.63069
3.62198
hayes−roth
5.64747
5.66068
5.65526
5.7202
5.70528
5.7244
Hill_Valley
0.61839
0.62463
0.62115
0.63662
0.65553
0.63397
hiv
1.15824
1.16435
1.1606
1.16142
1.16836
1.15938
imgRV
imgAL
imgAWO
isoRV
isoAL
isoAWO

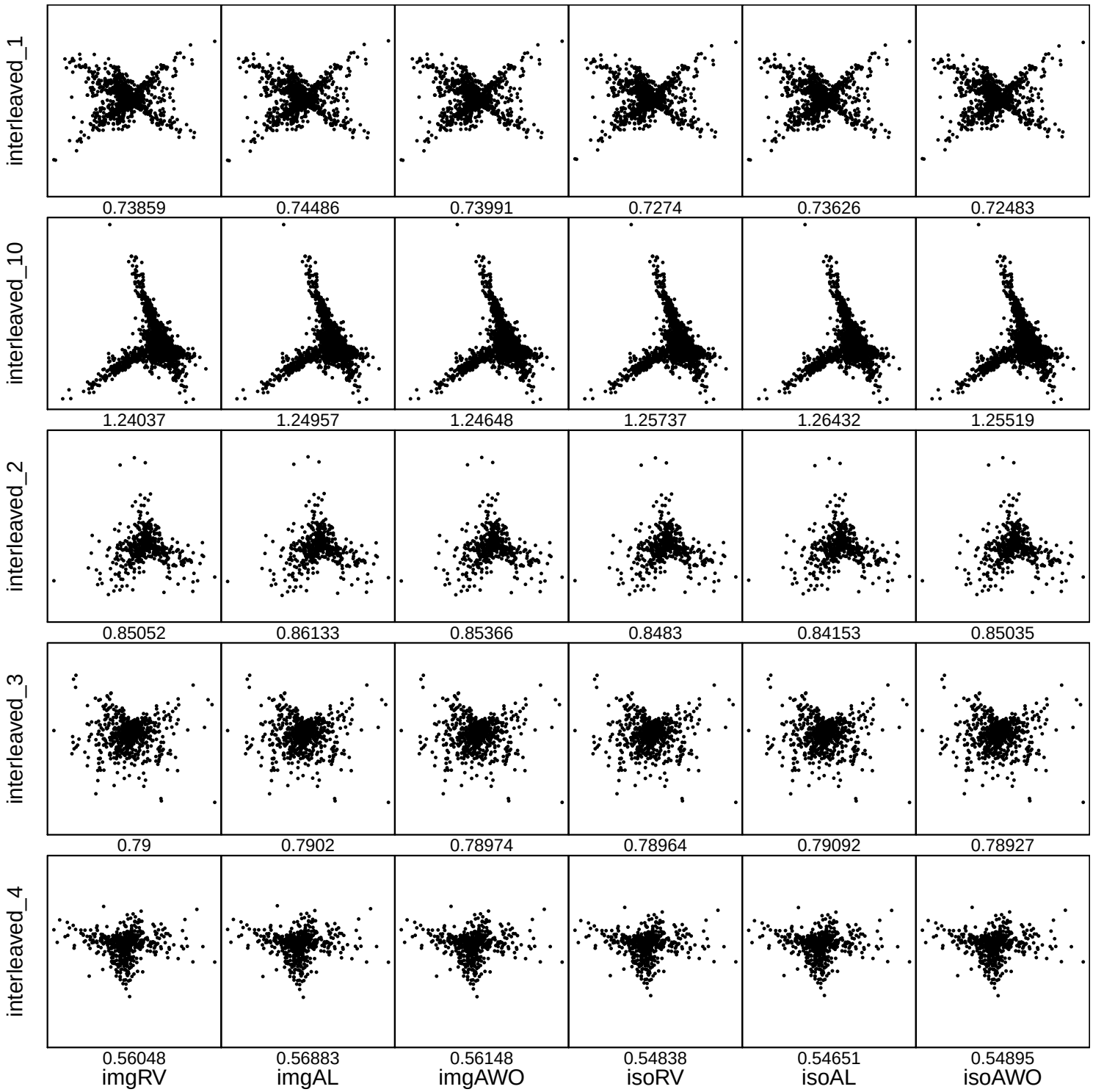
interleaved_1
0.73859
0.74486
0.73991
0.7274
0.73626
0.72483
interleaved_10
1.24037
1.24957
1.24648
1.25737
1.26432
1.25519
interleaved_2
0.85052
0.86133
0.85366
0.8483
0.84153
0.85035
interleaved_3
0.79
0.7902
0.78974
0.78964
0.79092
0.78927
interleaved_4
0.56048
0.56883
0.56148
0.54838
0.54651
0.54895
imgRV
imgAL
imgAWO
isoRV
isoAL
isoAWO

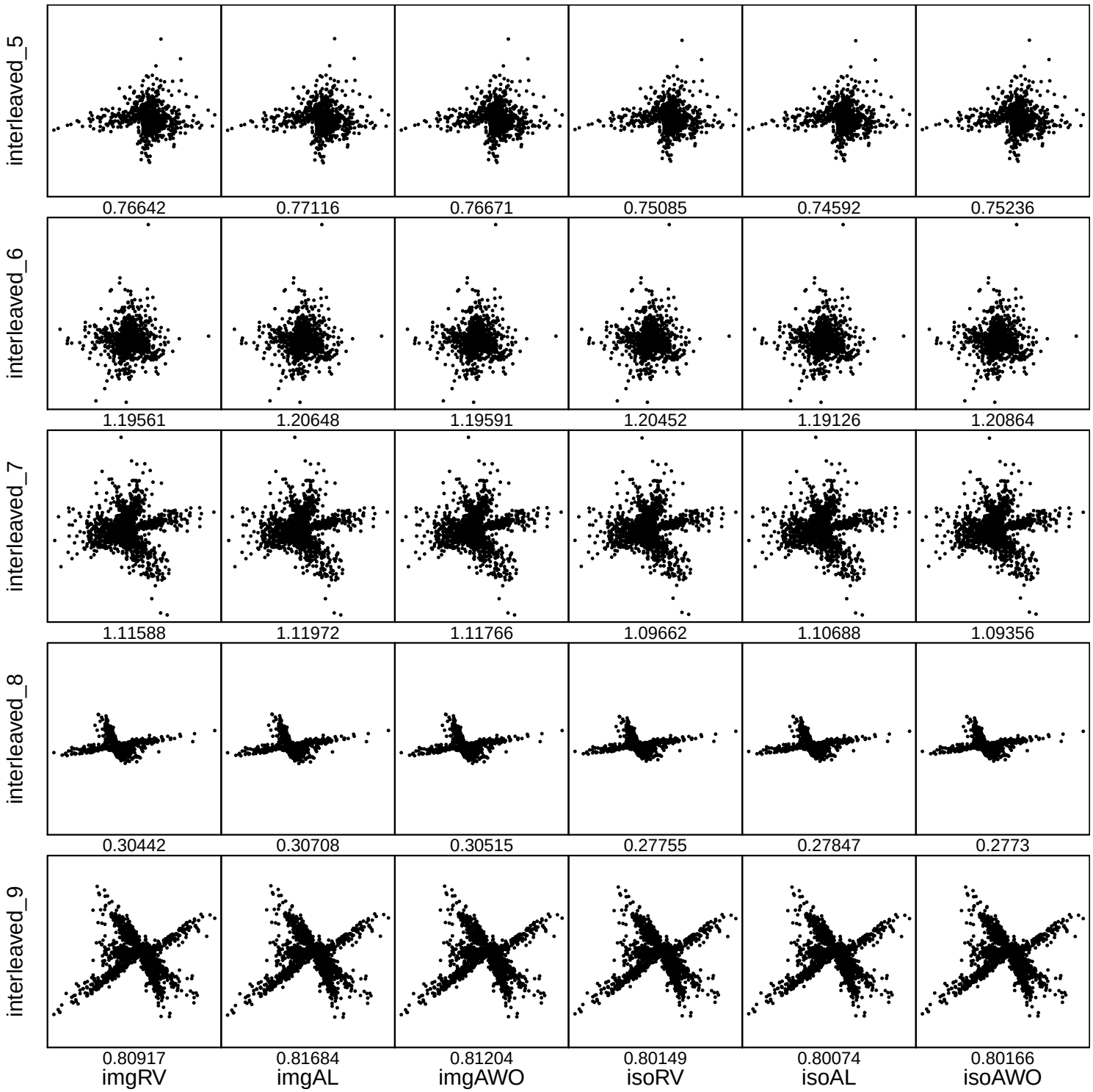
interleaved_5
0.76642
0.77116
0.76671
0.75085
0.74592
0.75236
interleaved_6
1.19561
1.20648
1.19591
1.20452
1.19126
1.20864
interleaved_7
1.11588
1.11972
1.11766
1.09662
1.10688
1.09356
interleaved_8
0.30442
0.30708
0.30515
0.27755
0.27847
0.2773
interleaved_9
0.80917
0.81684
0.81204
0.80149
0.80074
0.80166
imgRV
imgAL
imgAWO
isoRV
isoAL
isoAWO

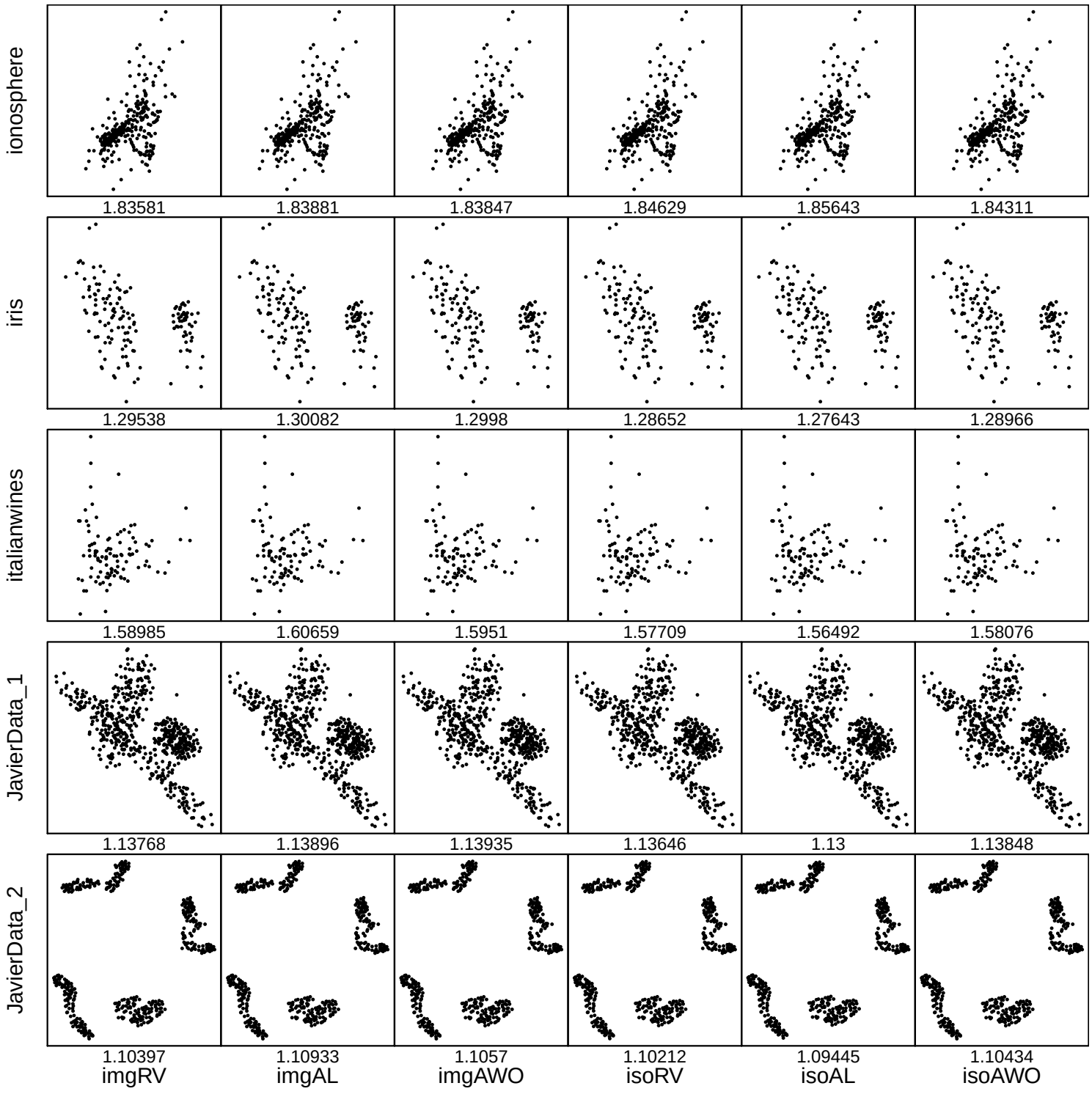
ionosphere
1.83581
1.83881
1.83847
1.84629
1.85643
1.84311
iris
1.29538
1.30082
1.2998
1.28652
1.27643
1.28966
italianwines
1.58985
1.60659
1.5951
1.57709
1.56492
1.58076
JavierData_1
1.13768
1.13896
1.13935
1.13646
1.13
1.13848
JavierData_2
1.10397
1.10933
1.1057
1.10212
1.09445
1.10434
imgRV
imgAL
imgAWO
isoRV
isoAL
isoAWO

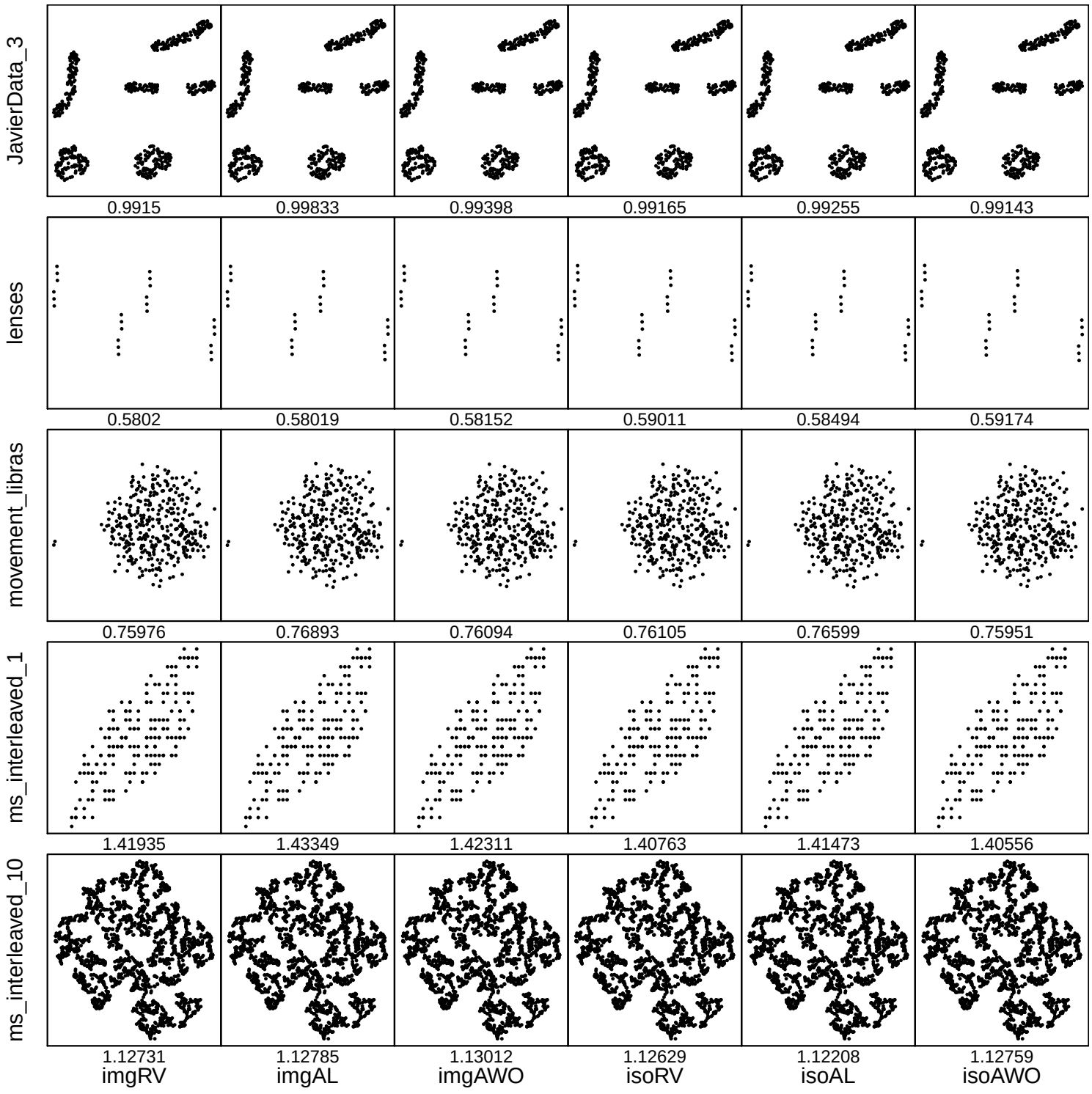
JavierData_3
0.9915
0.99833
0.99398
0.99165
0.99255
0.99143
lenses
0.5802
0.58019
0.58152
0.59011
0.58494
0.59174
movement_libras
0.75976
0.76893
0.76094
0.76105
0.76599
0.75951
ms_interleaved_1
1.41935
1.43349
1.42311
1.40763
1.41473
1.40556
ms_interleaved_10
1.12731
1.12785
1.13012
1.12629
1.12208
1.12759
imgRV
imgAL
imgAWO
isoRV
isoAL
isoAWO

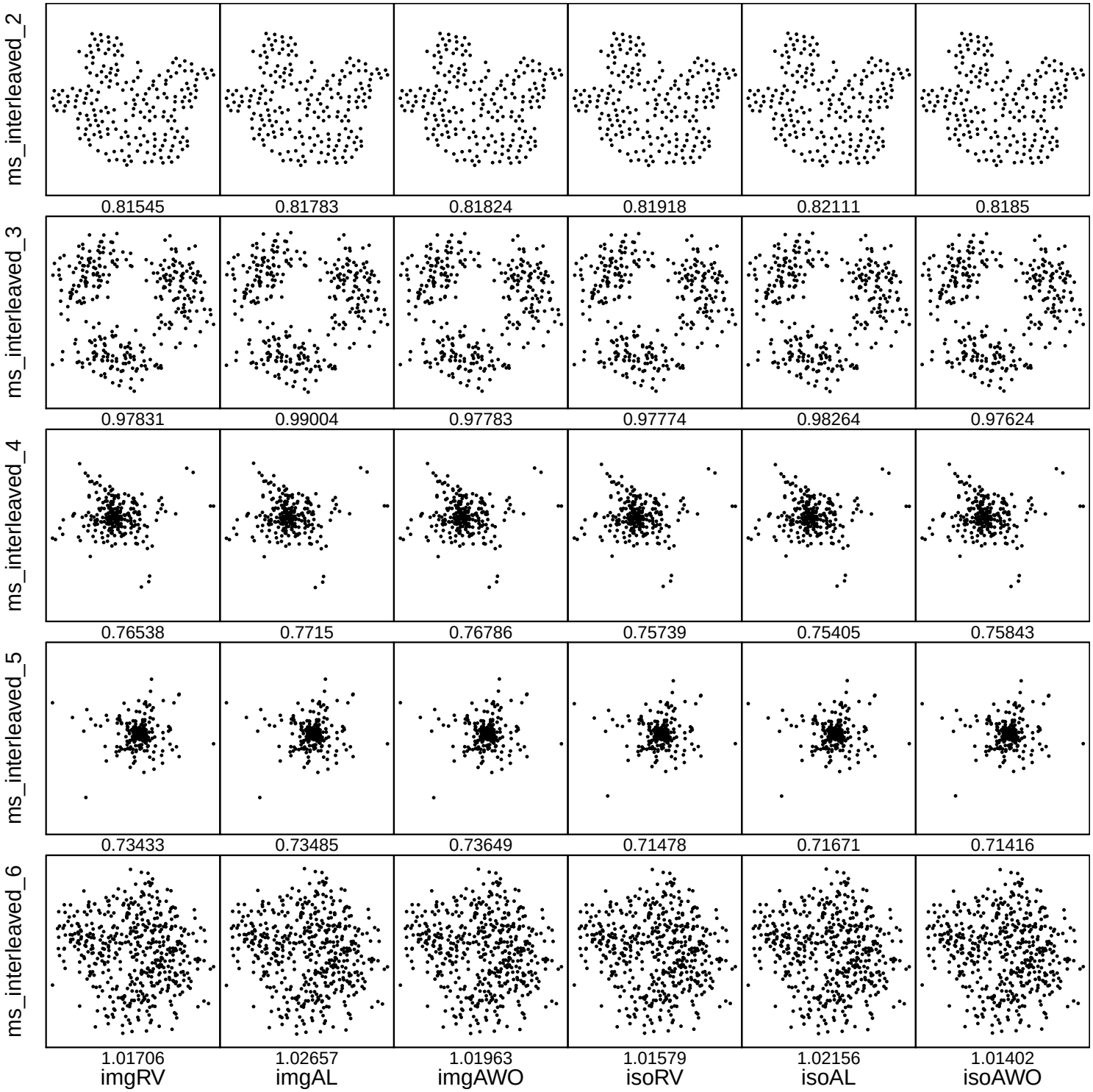
ms_interleaved_2
ms_interleaved_3
ms_interleaved_4
ms_interleaved_5
ms_interleaved_6
0.81545
0.81783
0.81824
0.81918
0.82111
0.8185
0.97831
0.99004
0.97783
0.97774
0.98264
0.97624
0.76538
0.7715
0.76786
0.75739
0.75405
0.75843
0.73433
0.73485
0.73649
0.71478
0.71671
0.71416
1.01706
1.02657
1.01963
1.01579
1.02156
1.01402
imgRV
imgAL
imgAWO
isoRV
isoAL
isoAWO

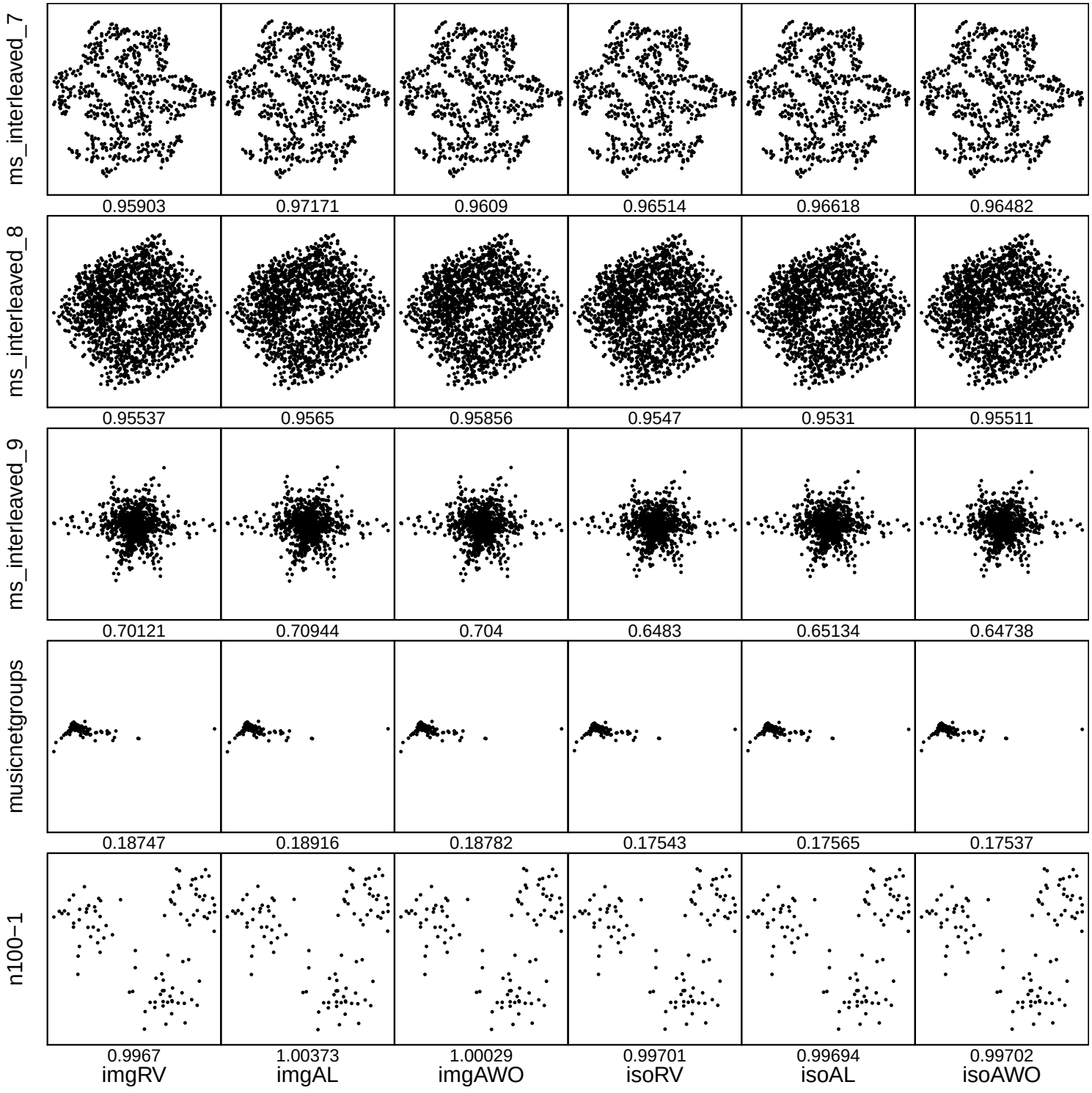
ms_interleaved_7
0.95903
0.97171
0.9609
0.96514
0.96618
0.96482
ms_interleaved_8
0.95537
0.9565
0.95856
0.9547
0.9531
0.95511
ms_interleaved_9
0.70121
0.70944
0.704
0.6483
0.65134
0.64738
musicnetgroups
0.18747
0.18916
0.18782
0.17543
0.17565
0.17537
n100−1
0.9967
imgRV
1.00373
imgAL
1.00029
imgAWO
0.99701
isoRV
0.99694
isoAL
0.99702
isoAWO

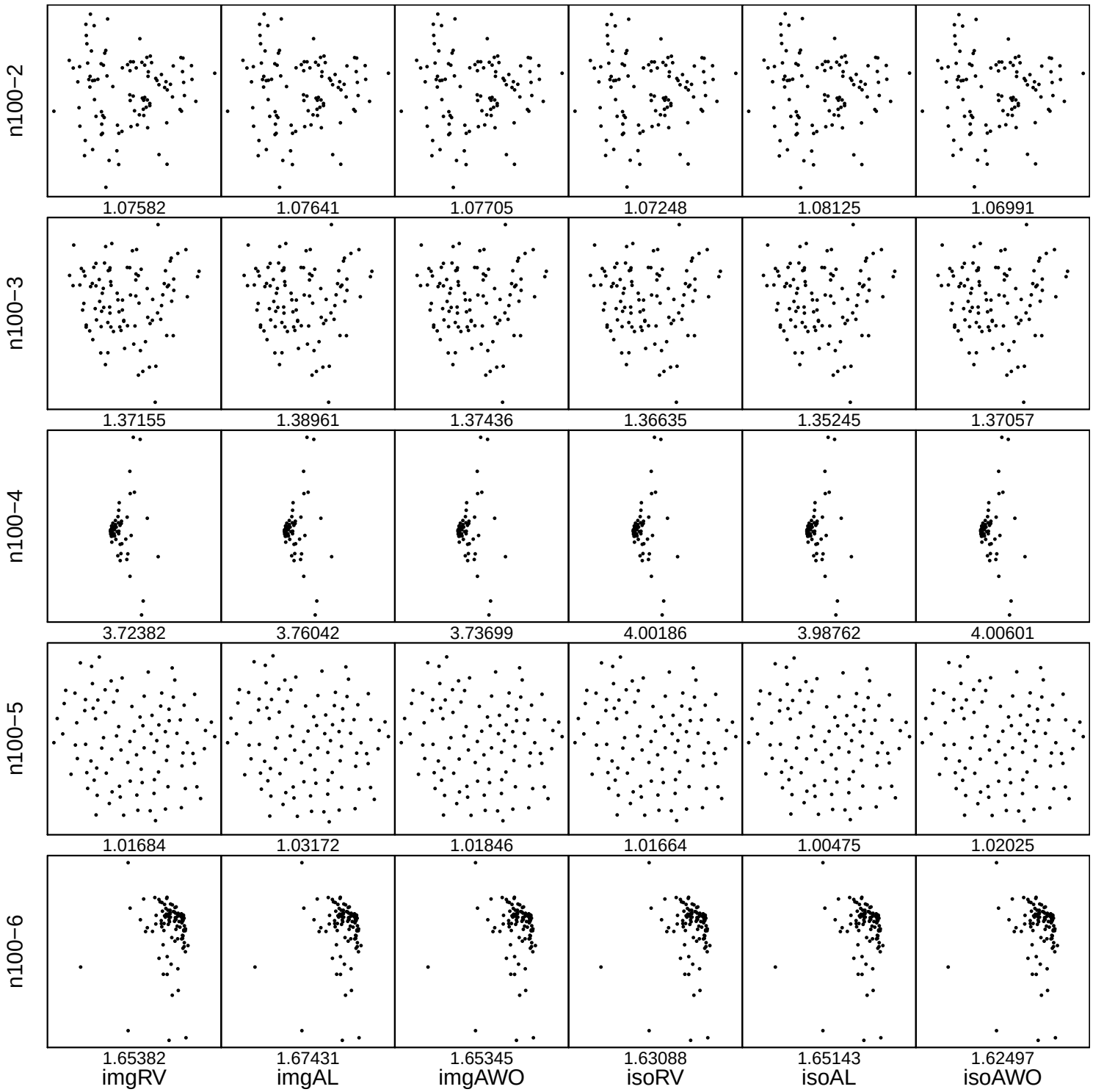
n100−2
n100−3
n100−4
n100−5
n100−6
1.07582
1.07641
1.07705
1.07248
1.08125
1.06991
1.37155
1.38961
1.37436
1.36635
1.35245
1.37057
3.72382
3.76042
3.73699
4.00186
3.98762
4.00601
1.01684
1.03172
1.01846
1.01664
1.00475
1.02025
1.65382
1.67431
1.65345
1.63088
1.65143
1.62497
imgRV
imgAL
imgAWO
isoRV
isoAL
isoAWO

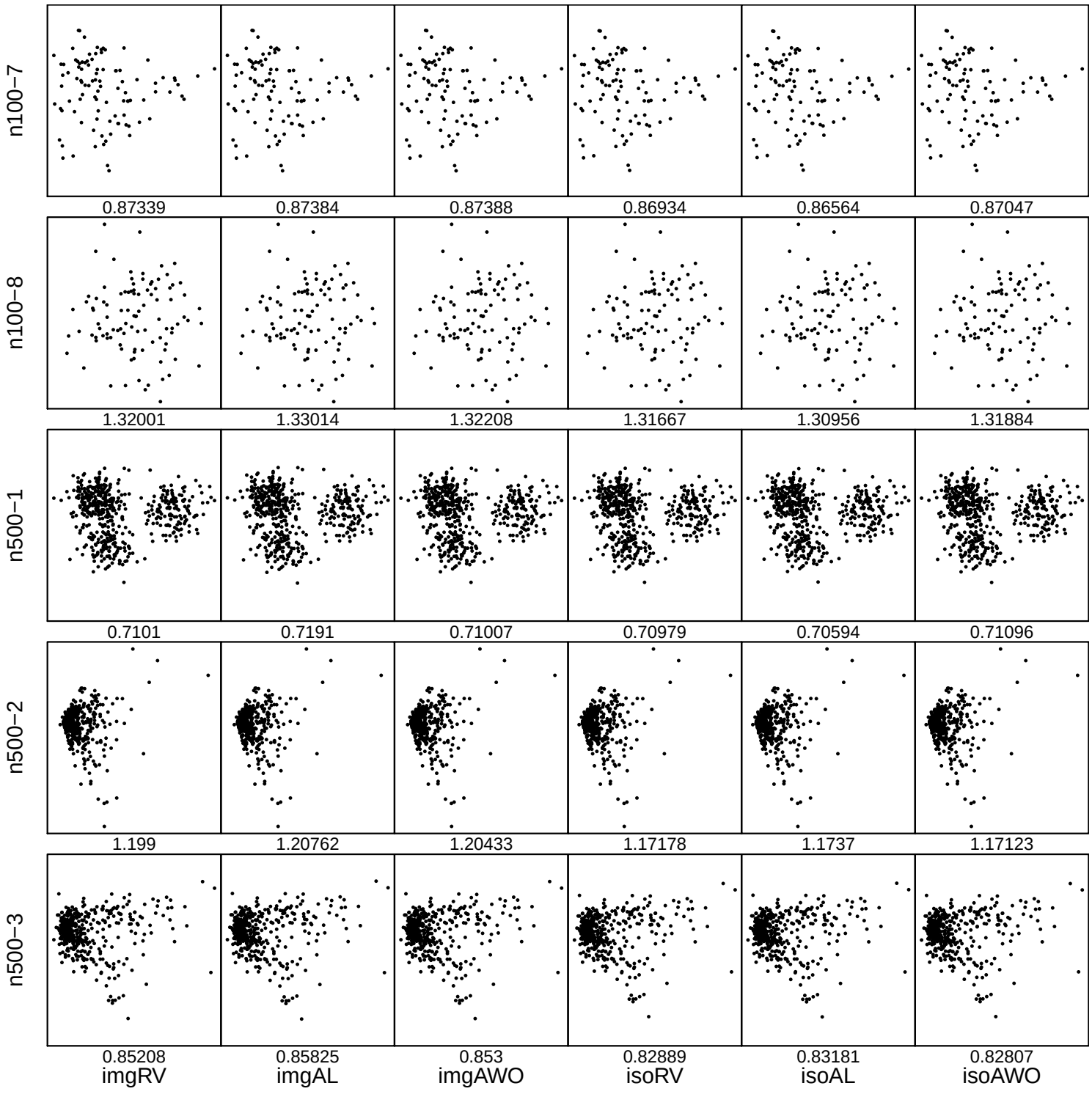
n100−7
n100−8
n500−1
n500−2
n500−3
0.87339
0.87384
0.87388
0.86934
0.86564
0.87047
1.32001
1.33014
1.32208
1.31667
1.30956
1.31884
0.7101
0.7191
0.71007
0.70979
0.70594
0.71096
1.199
1.20762
1.20433
1.17178
1.1737
1.17123
0.85208
0.85825
0.853
0.82889
0.83181
0.82807
imgRV
imgAL
imgAWO
isoRV
isoAL
isoAWO

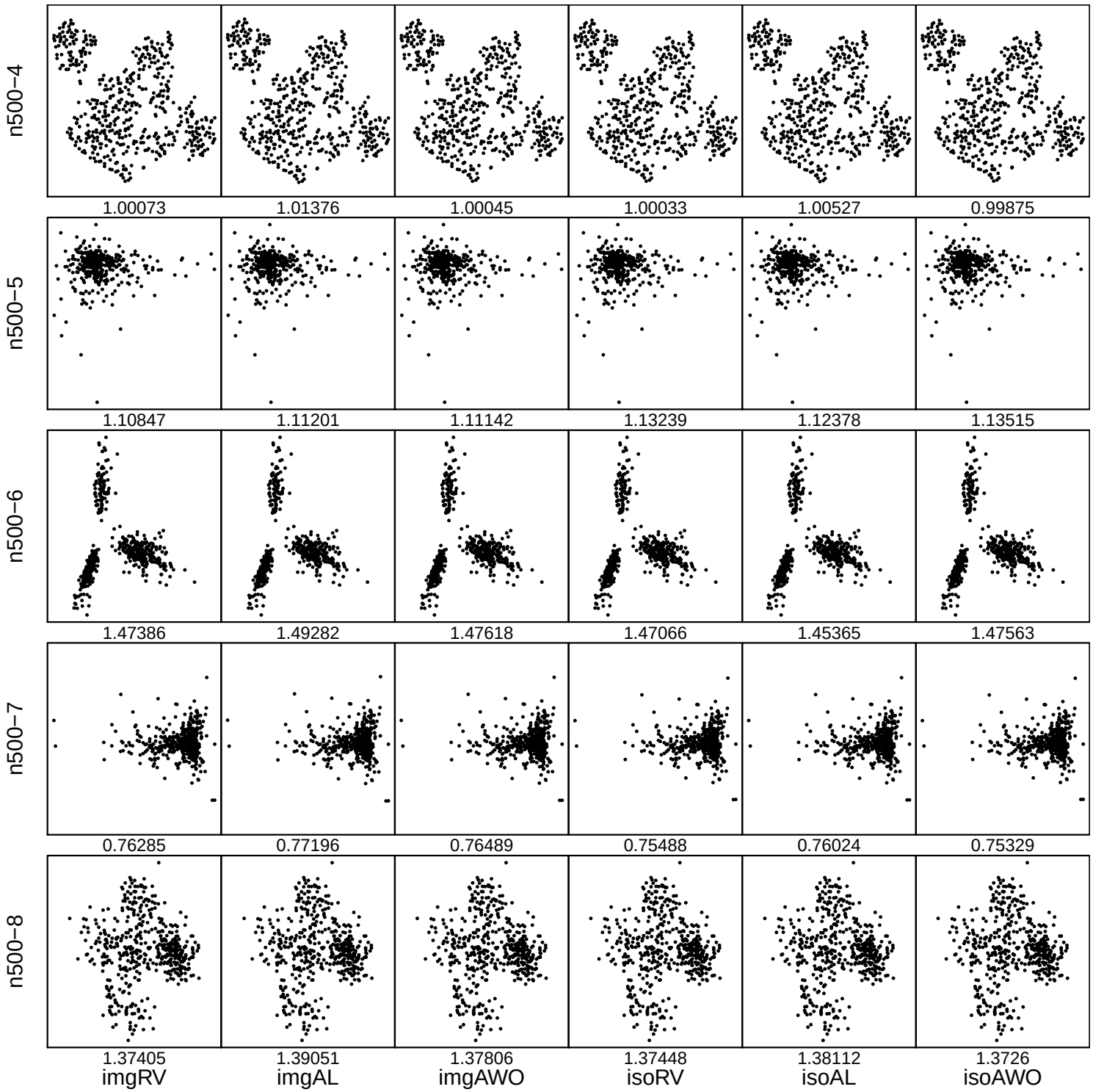
n500−4
n500−5
n500−6
n500−7
n500−8
1.00073
1.01376
1.00045
1.00033
1.00527
0.99875
1.10847
1.11201
1.11142
1.13239
1.12378
1.13515
1.47386
1.49282
1.47618
1.47066
1.45365
1.47563
0.76285
0.77196
0.76489
0.75488
0.76024
0.75329
1.37405
1.39051
1.37806
1.37448
1.38112
1.3726
imgRV
imgAL
imgAWO
isoRV
isoAL
isoAWO

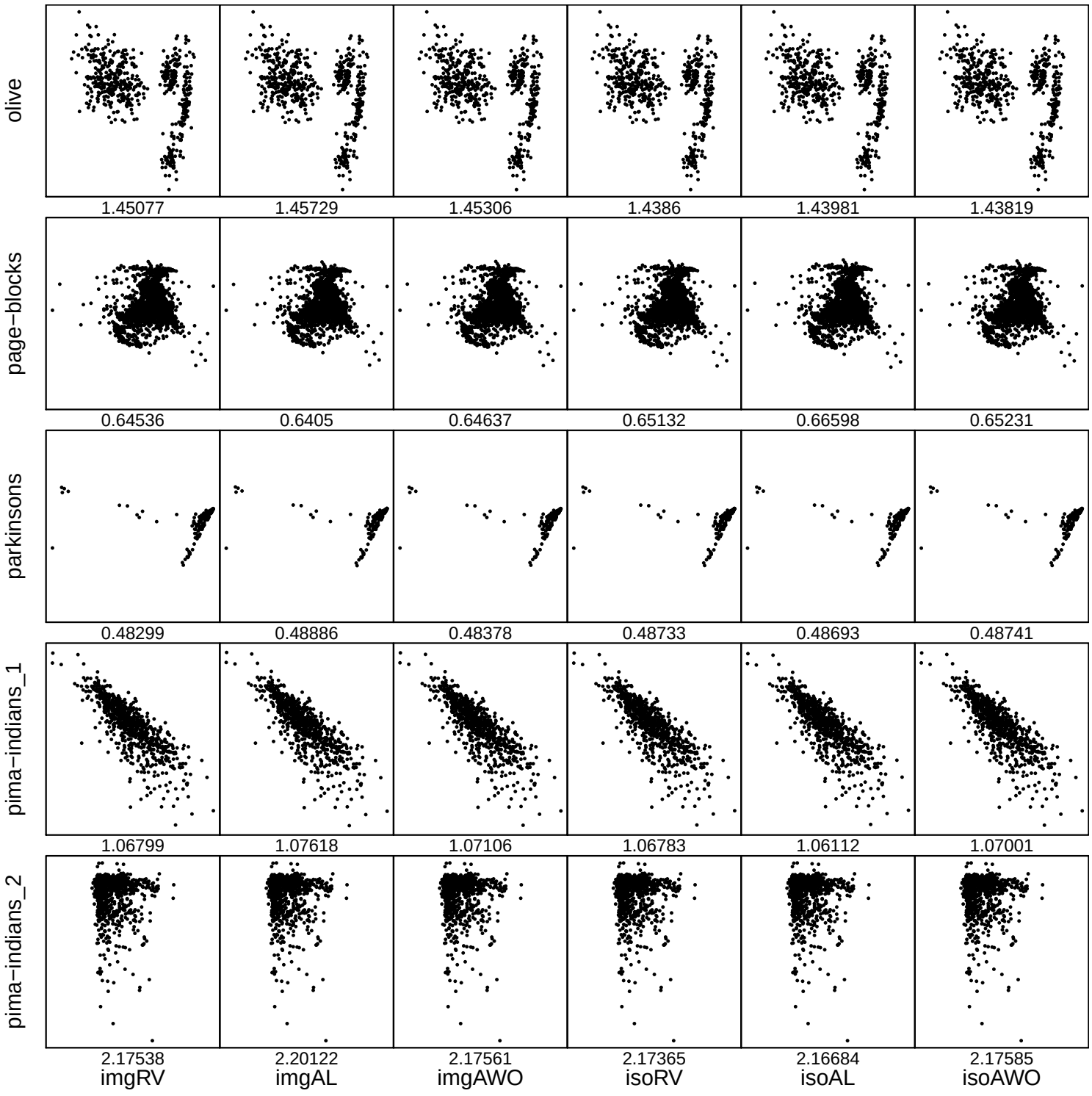
olive
1.45077
1.45729
1.45306
1.4386
1.43981
1.43819
page−blocks
0.64536
0.6405
0.64637
0.65132
0.66598
0.65231
parkinsons
0.48299
0.48886
0.48378
0.48733
0.48693
0.48741
pima−indians_1
1.06799
1.07618
1.07106
1.06783
1.06112
1.07001
pima−indians_2
2.17538
2.20122
2.17561
2.17365
2.16684
2.17585
imgRV
imgAL
imgAWO
isoRV
isoAL
isoAWO

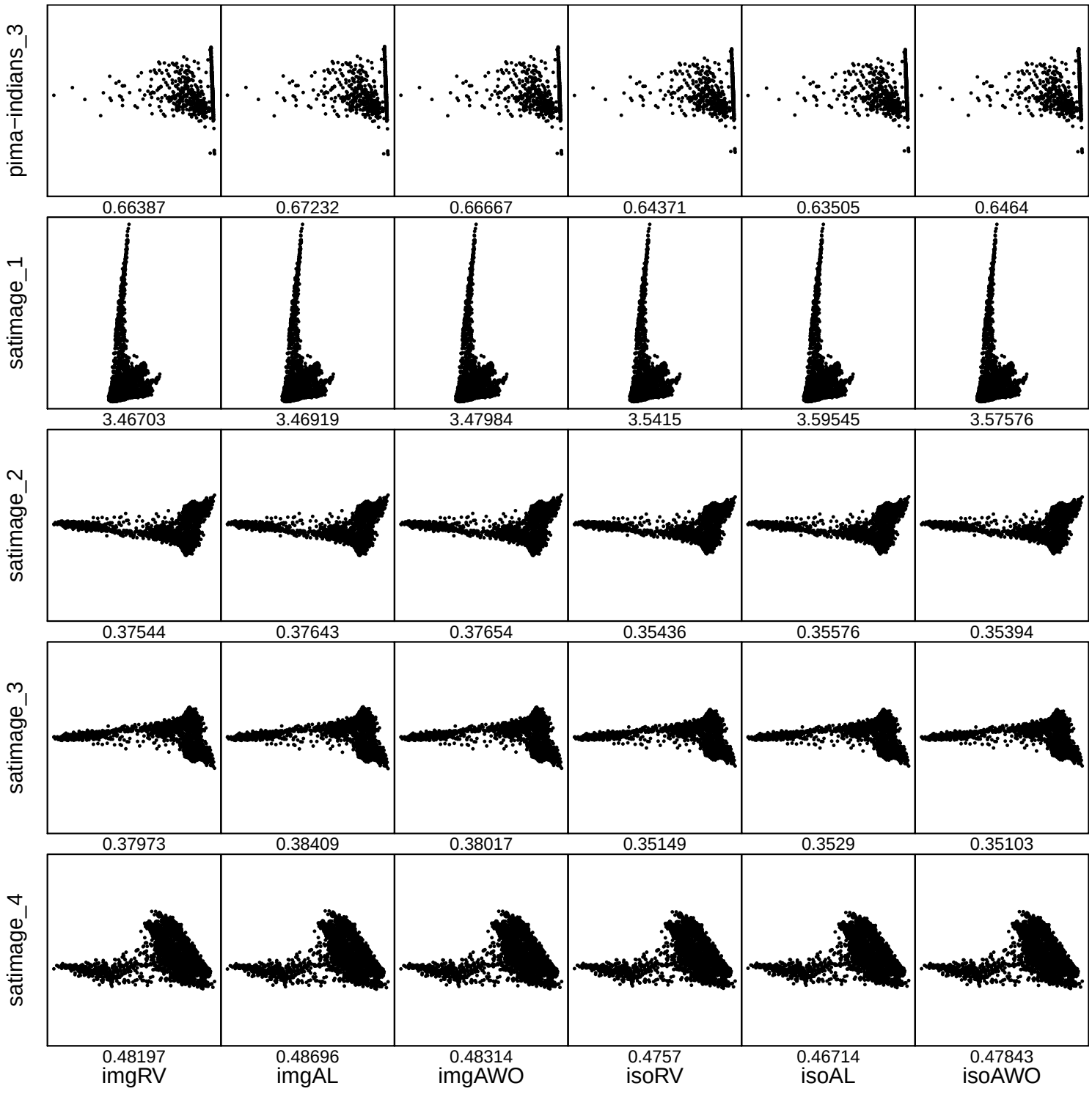
pima−indians_3
0.66387
0.67232
0.66667
0.64371
0.63505
0.6464
satimage_1
3.46703
3.46919
3.47984
3.5415
3.59545
3.57576
satimage_2
0.37544
0.37643
0.37654
0.35436
0.35576
0.35394
satimage_3
0.37973
0.38409
0.38017
0.35149
0.3529
0.35103
satimage_4
0.48197
0.48696
0.48314
0.4757
0.46714
0.47843
imgRV
imgAL
imgAWO
isoRV
isoAL
isoAWO

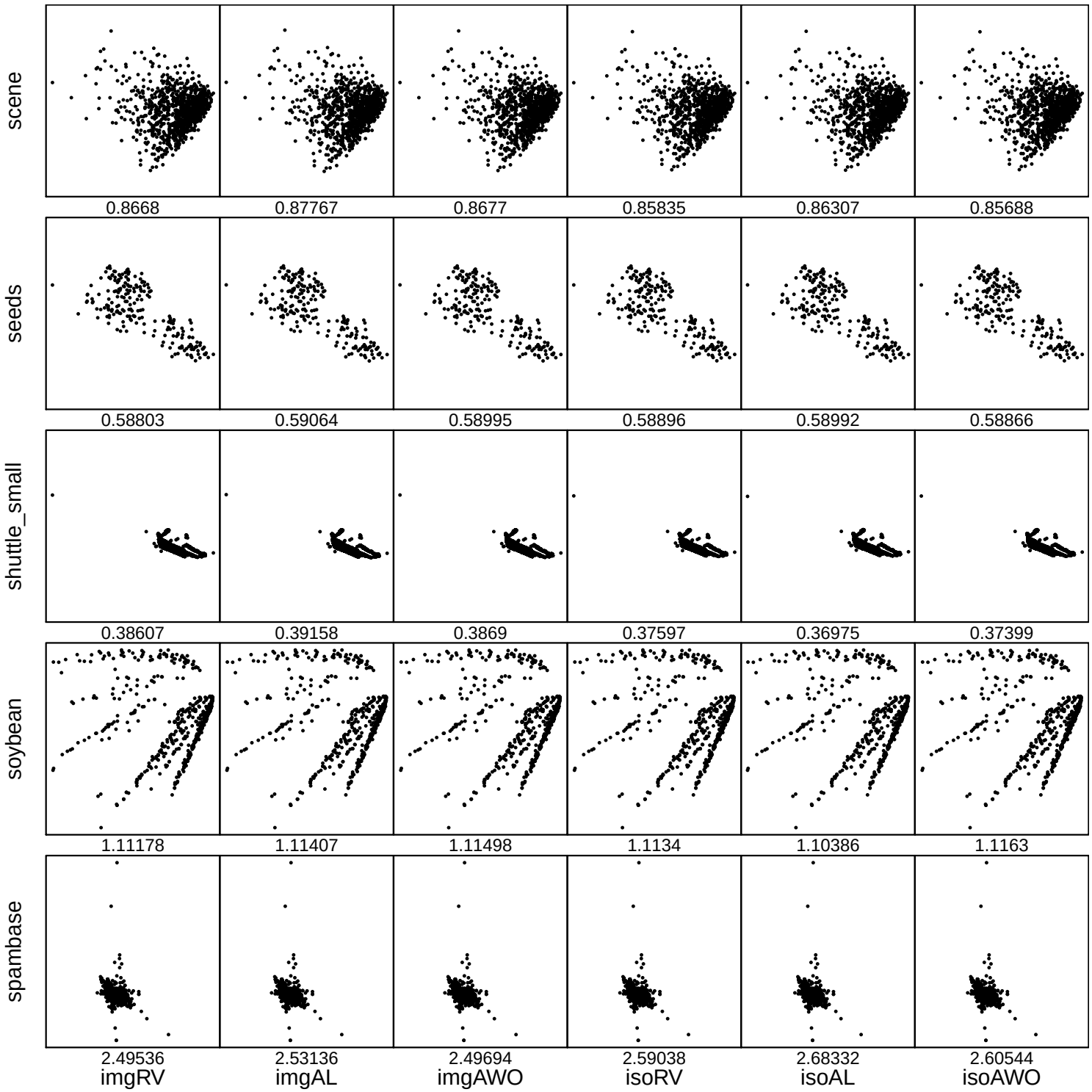
scene
seeds
shuttle_small
soybean
spambase
0.8668
0.87767
0.8677
0.85835
0.86307
0.85688
0.58803
0.59064
0.58995
0.58896
0.58992
0.58866
0.38607
0.39158
0.3869
0.37597
0.36975
0.37399
1.11178
1.11407
1.11498
1.1134
1.10386
1.1163
2.49536
2.53136
2.49694
2.59038
2.68332
2.60544
imgRV
imgAL
imgAWO
isoRV
isoAL
isoAWO

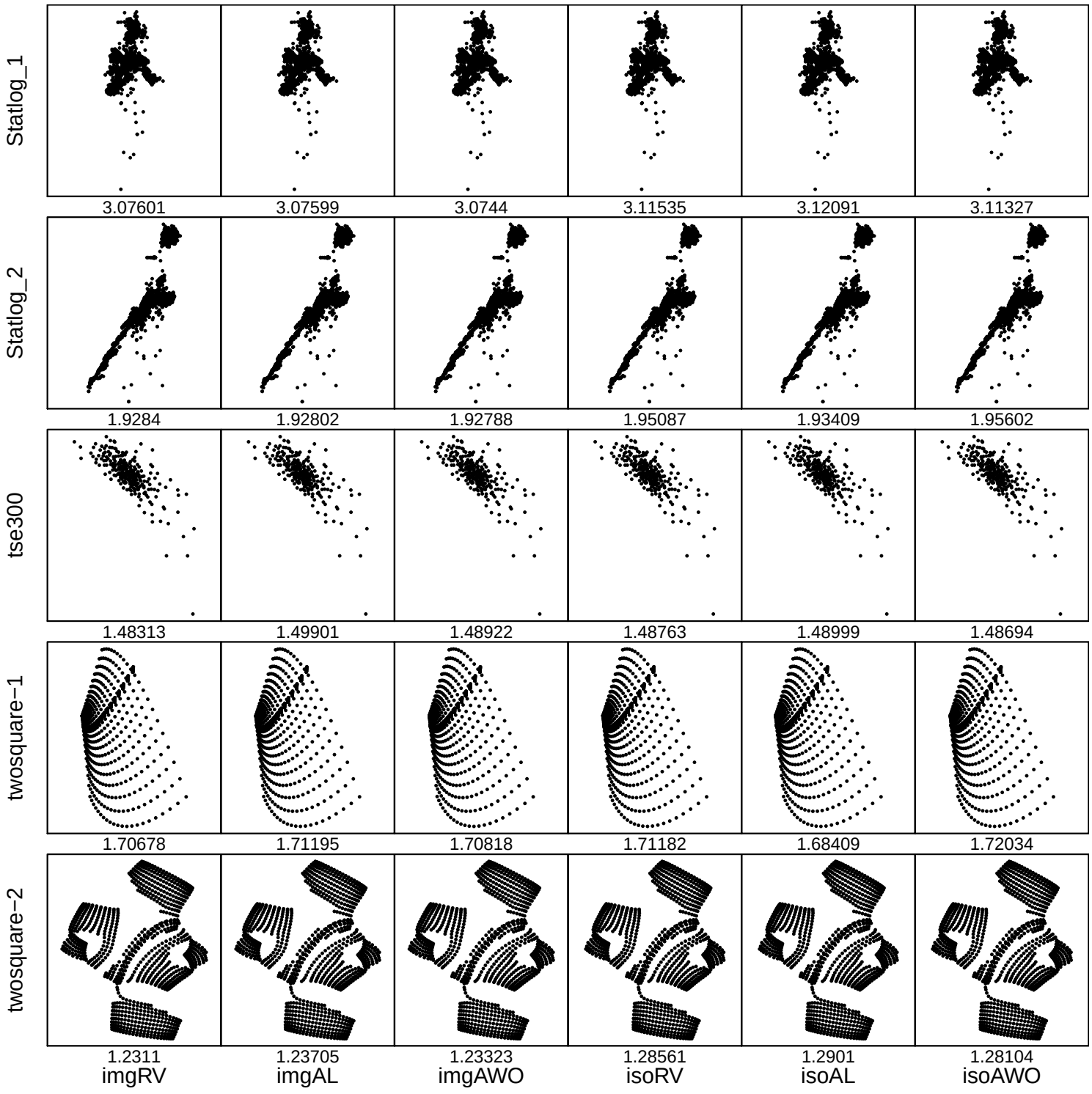
Statlog_1
3.07601
3.07599
3.0744
3.11535
3.12091
3.11327
Statlog_2
1.9284
1.92802
1.92788
1.95087
1.93409
1.95602
tse300
1.48313
1.49901
1.48922
1.48763
1.48999
1.48694
twosquare−1
1.70678
1.71195
1.70818
1.71182
1.68409
1.72034
twosquare−2
1.2311
1.23705
1.23323
1.28561
1.2901
1.28104
imgRV
imgAL
imgAWO
isoRV
isoAL
isoAWO

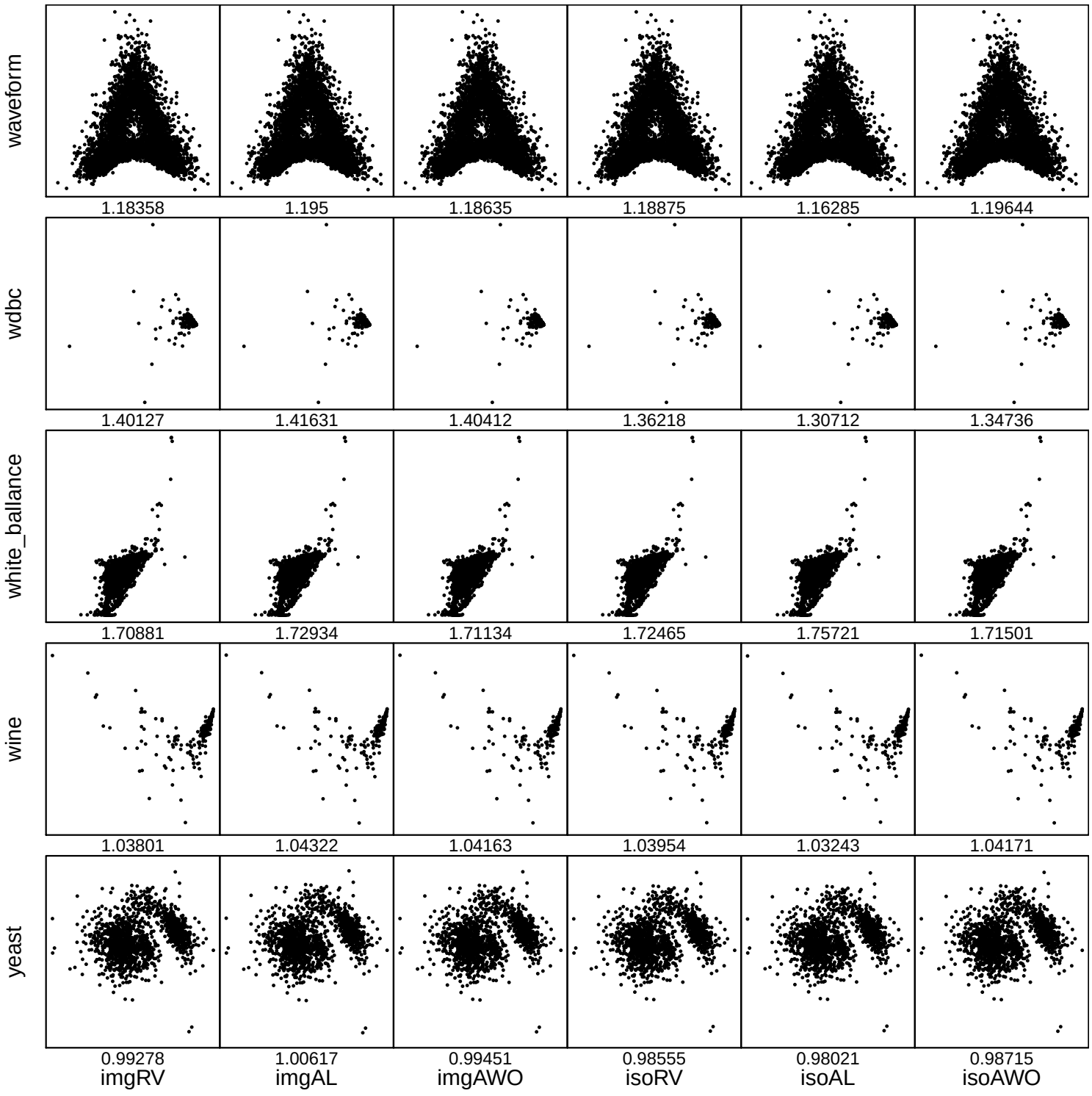
waveform
1.18358
1.195
1.18635
1.18875
1.16285
1.19644
wdbc
1.40127
1.41631
1.40412
1.36218
1.30712
1.34736
white_ballance
1.70881
1.72934
1.71134
1.72465
1.75721
1.71501
wine
1.03801
1.04322
1.04163
1.03954
1.03243
1.04171
yeast
0.99278
1.00617
0.99451
0.98555
0.98021
0.98715
imgRV
imgAL
imgAWO
isoRV
isoAL
isoAWO

REFERENCES

[1] S. Bachthaler and D. Weiskopf. Continuous scatterplots. *IEEE Trans. Vis. & Comp. Graphics*, 14(6):1428–1435, 2008.

[2] M. Bostock. Multi-series line chart. https://bl.ocks.org/mbostock/3884955. Accessed February 24, 2018.

[3] D. Dawson and K. Reid. Fatigue, alcohol and performance impairment. *Nature*, 388(6639):235, 1997.

[4] D. Dheeru and E. Karra Taniskidou. UCI machine learning repository, 2017. http://archive.ics.uci.edu/ml.

[5] M. Fink, J.-H. Haunert, J. Spoerhase, and A. Wolff. Selecting the aspect ratio of a scatter plot based on its Delaunay triangulation. *IEEE Trans. Vis. & Comp. Graphics*, 19(12):2326–2335, 2013.

[6] K. J. Gaston. Global patterns in biodiversity. *Nature*, 405(6783):220, 2000.

[7] C. Johnson. Species extinction and the relationship between distribution and abundance. *Nature*, 394(6690):272, 1998.

[8] V. I. S.-B. W. S. Network. Typical day at shawnigan lake. http://www.victoriaweather.ca/typicalday.php?id=132. Accessed February 13, 2012.

[9] M. Sedlmair, A. Tatu, T. Munzner, and M. Tory. A taxonomy of visual cluster separation factors. *Computer Graphics Forum*, 31(3):1335–1344, 2012.

[10] J. Talbot, J. Gerth, and P. Hanrahan. Arc length-based aspect ratio selection. *IEEE Trans. Vis. & Comp. Graphics*, 17(12):2276–2282, 2011.

[11] W. Volkmuth and R. Austin. DNA electrophoresis in microlithographic arrays. *Nature*, 358(6387):600, 1992.

[12] Y. Wang, J. Zhang, D. J. Lehmann, H. Theisel, and X. Chi. Automating transfer function design with valley cell-based clustering of 2D density plots. *Computer Graphics Forum*, 31(3):1295–1304, 2012.